Appl. Phys. A (2015) 121:915–938
DOI 10.1007/s00339-015-9456-x

Applied Physics A
Materials Science & Processing

INVITED PAPER

Cinnabar alteration in archaeological wall paintings: an experimental and theoretical approach

Madeleine Kegelman Neiman[1] · Magdalena Balonis[2,3] · Ioanna Kakoulli[4,5]

Received: 1 March 2015 / Accepted: 28 August 2015 / Published online: 8 September 2015

Abstract The red mineral pigment known as cinnabar (HgS) was commonly employed in Roman *fresco* wall paintings. *Fresco* artists of the period favored this pigment for its striking red color. However, upon excavation and exposure to air and light, cinnabar-pigmented surfaces recovered from archaeological contexts often proved to be unstable. Mural paintings colored with cinnabar that have been exposed in the open air frequently demonstrate a disfiguring, irreversible darkening of the surface. Traditionally, scholars have attributed this alteration to a light-induced phase change from red α-cinnabar to black β-cinnabar (meta-cinnabar). While this transformation has not been totally excluded, the prevailing view among conservation scientists is that chlorine plays a key role in the darkening process through the formation of light-sensitive mercury chloride compounds, or as a catalyst in the photochemical redox of Hg(II)S into Hg(0) and S(0). Using laboratory-based experiments and thermodynamic modeling, this paper attempts to further clarify the mechanism(s) and kinetics of cinnabar alteration in *fresco* applications, especially the role of light, humidity, and chlorine ions. Additionally, it explores possible pathways and preventive as well as remedial conservation treatments during or immediately following excavation, to inhibit or retard darkening of cinnabar-pigmented *fresco* surfaces.

✉ Magdalena Balonis
magdalena.balonis@gmail.com

[1] UCLA-Getty Conservation Program, University of California, 308 Charles E. Young Drive North, A210 Fowler Building, Los Angeles 90095, CA, USA

[2] Department of Materials Science and Engineering, University of California, 410 Westwood Plaza, 2121K Engineering V, Los Angeles 90095, CA, USA

[3] Institute for Technology Advancement, University of California, Engineering VI, Los Angeles 90095, CA, USA

[4] Department of Materials Science and Engineering, University of California, 410 Westwood Plaza, 3111 Engineering V, Los Angeles 90095, CA, USA

[5] UCLA/Getty Conservation Program and Cotsen Institute of Archaeology, University of California Los Angeles, 308 Charles E. Young Drive North, A210 Fowler Building, Los Angeles, CA 90095, USA

1 Introduction

Within the Roman World, mural paintings adorned both public and private spaces [1–3]. The walls of *lararia* (sacred place of affluent Roman homes), tombs, and shop-façades were decorated with wall paintings depicting architectural vignettes and panoramic landscapes, as well as scenes displaying daily life, historic events, and mythic tales [4–6]. These mural paintings serve as a cultural record of the ancient world; a testament to the technical and artistic skills of their creators, as well as a visual chronicle of the society's religious, economic, and social history. The study of archaeological wall paintings across the Mediterranean offers scholars an important point of entry into understanding ancient Roman culture and society.

While the excavation of ancient wall paintings has been a boon for archaeologists and art historians, the change in microclimate prompted by their unearthing induces—in many cases—new and accelerated degradation processes. Excavation disrupts the equilibrium of the burial environment spurring increased rates of decay. Once exposed, wall paintings are subject to chemical, mechanical, and biological deterioration [7–11]. The presence of salts, exposure to visible and ultraviolet light, pollution, microbiological activity and moisture, all contribute to the

degradation of wall paintings generally and the pigmented surface in particular [7–15]. One of the most complex and challenging degradation processes in wall painting is color alteration. Shifts in hue, value or chroma, darkening or complete color transformation are not only visually disruptive and obscure the artist's intent, but they also change the meaning and chemical stability of the painting.

The darkening of cinnabar (HgS) pigment, in particular, has been one of the most common and puzzling color alterations in wall paintings. The phenomenon was first described and recorded in antiquity by Roman scholars who witnessed their paintings pigmented with cinnabar rapidly change from red to black. Pliny the Elder notes during the first century A.D. in his work *Nauralis Historia* that "exposure to the light, either of sun or the moon, is injurious to the color" [16]. Another Classical author Vitruvius who also wrote about Greek and Roman art and architecture describes in his book *De Architectura* the application of a wax coating over areas painted with cinnabar to prevent it from darkening [17]. In modern times, cultural heritage professionals at the Roman site of Pompeii, Italy, and at other archaeological sites where wall painting are pigmented with cinnabar have also reported the same phenomenon, red paint layers darken significantly after excavation [18, 19].

Traditionally, scholars have attributed cinnabar alteration to a light-induced conformational change from red α-cinnabar (HgS trigonal) to black β-cinnabar (meta-cinnabar, HgS cubic) [20–24] leading to the assumption that a shift in the crystal structure was responsible for the color change. However, the more recent use of highly sensitive microanalytical techniques, including Raman spectroscopy, as well as synchrotron-based techniques such as X-ray diffraction (SR-μXRD) and X-ray absorption near-edge structure (SR-μXANES), has not supported this hypothesis. To this date, meta-cinnabar has only been identified within altered cinnabar on one cultural heritage object; Istudor [25] detected meta-cinnabar in wall paintings at the sixteenth century Sucevița monastery. Additionally, a review of the geochemical literature suggests that transformation from α-cinnabar to β-cinnabar requires application of significant thermal energy; α-cinnabar must be heated to an excess of 381 °C to cause a phase change [26].[1] This stands in contrast to anecdotal and empirical accounts that describe cinnabar alteration under ambient conditions [19, 27–30]. While the theory is largely considered outmoded, it continues to be cited within the literature as a possible means of explaining the blackening of cinnabar [31].

More recently, conservation science has drawn from geochemical research showing that halogen impurities, in particular chlorine (Cl), are responsible for the photosensitivity of cinnabar [27, 28, 32, 33].[2] McCormak et al. [32] demonstrated that exposure of cinnabar to halide solution will induce photosensitivity of the ore. McCormak [27] examined the samples of naturally occurring photosensitive and non-photosensitive cinnabar gleaned from mines across the globe using microprobe analysis; the study found that only the photosensitive ores contained chlorine. Analysis of cultural heritage materials has shown a similar correlation between the presence of chlorides and blackening of cinnabar in oil and tempera canvas paintings, as well as *frescoes*. In these studies, scholars have identified the presence of mercury chloride-containing compounds in the blackened areas [19, 23, 29, 30, 34–37].

While conservation scientists now largely agree that chlorine plays a key role in the alteration process, specific mechanism by which this occurs remains ambiguous. Scholars have posited two possible pathways by which chlorine might provoke a light-induced alteration. In the first, chlorine reacts with cinnabar to form various light-sensitive mercury chloride and mercury sulfochloride compounds [19, 23, 35, 36, 38]. Analysis of blackened cinnabar on cultural heritage materials has identified presence of calomel (Hg_2Cl_2) as well as $Hg_3S_2Cl_2$ polymorphs including corderoite (α-$Hg_3S_2Cl_2$), β-$Hg_3S_2Cl_2$, and kenhsuite (γ-$Hg_3S_2Cl_2$) [36]. Presence of such compounds could certainly alter the color of surface as Cotte et al. [19] and Radepont et al. [36] suggest; calomel and corderoite in particular are grayish in color. To our knowledge, however, there is no known mercury chloride-containing compound that would account for the black color observed. A second pathway for the transformation is described by Keune and Boon [34] who proposed that chlorine serves as a catalyst for photochemical redox reaction of Hg(II)S into Hg(0) and S(0). They posit that nanoparticles of colloidal Hg(0)—metallic mercury—deposited on the remaining intact HgS surface result in the blackened appearance. The presence of Hg–Cl compounds is explained by the subsequent reaction of Hg(0) with excess chloride ions. It should be noted, however, that while they were able to identify mercury chloride-containing compounds, the presence of metallic mercury could not be conclusively proven. Though detecting metallic mercury via experimental methods is technically challenging, the possibility for Hg(0) formation has been

[1] The presence of zinc or iron has been shown to reduce the temperature of transformation, to 204 and 305 °C, respectively. While substantially lower, the temperature required to induce this phase change still remains quite high.

[2] While chlorine has been the most thoroughly explored, other halogens, namely iodine, have also been shown to trigger the blackening of cinnabar.

demonstrated through electrochemical [39] and more recently thermodynamic modeling approaches [37].

The formation of a sulfate-based compound, more specifically gypsum, has also been suggested as a possible source of darkening on cinnabar-pigmented *frescoes*. Presence of black gypsum crusts on a variety of calcareous surfaces including limestone, marble, and wall paintings due to SO_2 pollution is well documented within the conservation literature [40–47]. Gypsum has been detected in areas of altered cinnabar on *fresco* wall painting samples recovered from Pompeii [19, 29, 36] and Santa Maria Church in Northern Spain [48]. However, as noted above, cinnabar alteration has been observed on a range of artworks including oil and tempera paintings as well as on the ore itself. Presence of calcium carbonate is not required for cinnabar to darken. Therefore, while black gypsum crusts on some cinnabar-pigmented wall paintings have likely contributed to the darkening, they cannot be considered responsible for the light-induced blacking of cinnabar.

The exact source of chlorine within cinnabar in archaeological *fresco* paintings, as well as the method and time of its introduction, remains obscure. Chlorine-bearing compounds, including mercury chloride and mercury sulfochloride such as corderoite and calomel, have been found to coexist with cinnabar in geological contexts [29]. Chlorine contamination might have therefore occurred during processing of the pigment prior to use. The Roman architect Vitruvius wrote in the first century B.C.: "When the lumps of ore are dry, they are crushed in iron mortars and repeatedly washed and heated until impurities are gone and the colors come" [17]. Cotte et al. [19] have also suggested that Punic wax, a protective coating applied to *fresco* surfaces in antiquity, might have served as the source of chlorine. According to Pliny, "Punica wax is made this way: yellow beeswax is often exposed to air for a long time, then it is boiled in water from high sea, to which added nitre. Then, wax bloom is removed with a spoon, e.g. the whitest part, and is poured into a pot containing a bit of cold water, this part is boiled again in seawater, an then the vas is cold" [16]. However, in wall paintings, it is most likely that chlorine-containing compounds from the vicinity of seawater, within the soil or groundwater have served as the source of contamination.

In view of currently existing knowledge gaps, using laboratory-based experiments to simulate real case scenarios and thermodynamic modeling to understand phase equilibria, this study attempts to further investigate the mechanism(s) and kinetics of cinnabar alteration in *fresco* paintings and more specifically the role of light, humidity, and chlorine ions in the color change of the pigment. Additionally, it explores possible pathways through preventive (protection of the painted surface from sunlight) and remedial conservation treatments (desalination) during or immediately following excavation, to inhibit or retard darkening of cinnabar-pigmented *fresco* surfaces.

2 Materials and methods

2.1 *Fresco* and *secco* techniques

In Classical antiquity, two different techniques were used for painting on walls: *fresco* and *secco*. *Fresco* technique refers to any painting executed on a moist calcium hydroxide (lime)-rich plaster layer. The pigments are applied with water and are fixed by the formation of a carbonate lattice during the setting of the lime based on Reaction 1.

$$\underset{\text{Slaked lime}}{Ca(OH)_2} + CO_2 \rightarrow \underset{\text{Carbonated lime}}{CaCO_3} + H_2O \uparrow$$

The setting of lime is based on a chemical reaction between the calcium hydroxide ($Ca(OH)_2$) and the carbon dioxide (CO_2) of the atmosphere.

Owing to the high alkalinity of the lime and the exothermic reaction during setting, only a small number of pigments are compatible with the *fresco* technique.

Secco technique involves no chemical reaction for the fixing of the pigments. As suggested by the etymology of the word ("secco" means "dry" in Italian), *secco* painting involves the use of dry plaster or whitewash, onto which the pigments are fixed by the use of a film-forming organic binding medium such as egg, siccative oil, gum, and others. This technique is, therefore, not restricted to lime plasters. Plaster layers can involve also clay, gypsum, or calcium carbonate as the principle plaster binders. In many cases, the painting is executed directly on the support (rock-cut surface, stone blocks).

2.2 Preparation of cinnabar-pigmented *fresco* mock-up blocks

Fresco mock-ups were fabricated by combining commercial calcium hydroxide (lime putty) binder, Carrera marble dust (0.2–0.6 mm) aggregate, and deionized water in a 1:3:1 volumetric ratio [31] imitating the methods of application in Classical antiquity. Lime putty and marble dust were purchased from Kremer Pigments Inc.

Dense mortar was decanted into custom-made stainless steel molds (5 cm × 5 cm × 2 cm) and allowed to dry for approximately 2 h. Damp surface was then painted with a fluid mixture of 2:1 w/v natural cinnabar and deionized water. Natural cinnabar pigment which originated from China was purchased from Kremer Pigments Inc., USA, and its phase composition was checked through the XRD measurement. Absence of chlorine was

confirmed via XRF analysis. Chlorine strip test was performed on the DI water and did not reveal any presence of Cl^-. Blocks were subsequently left to dry in the dark under laboratory ambient conditions (23–26 °C and ~35 ± 5 % RH) for 1 week; at that time, they were unmolded and allowed to carbonate for not less than 6 weeks.

2.3 Accelerated artificial discoloration

In order to artificially reproduce the alteration observed in archaeological *frescoes*, laboratory-produced mock-up blocks were first infused with sodium chloride (NaCl) solutions of different molarities via capillary action and subsequently exposed to light.

Keeping the mock-ups in a dark chamber to avoid light exposure, a low (0.1 M) and a high concentration (5 M) of sodium chloride (NaCl) solution replicated the extremes of salinity that could be found within a *fresco* unearthed from an archaeological context where Cl^- is introduced via capillary impregnation. For this experiment, a single layer of glass beads was spread across the base of a petri dish, and the *fresco* mock-up blocks were placed on the beads with the paint surface down. The salt solution was slowly pipetted into the dish until in level with the painted surface, allowing the salt solution to be transferred through the block by capillary action. Blocks were left in contact with the saline solution for approximately 12 h. The pH of the saline solution at the beginning and the end of the infusion period was recorded with a Merck© pH strip. An indicator strip was dipped into the solution at hour 0 and at hour 12.

2.4 Light exposure

The mock-up blocks were subsequently exposed to sunlight. Published literature attributes the cinnabar darkening to ultraviolet and visible light wavelengths. However, no evidence-based study has resolved which exact part of the electromagnetic radiation is responsible for the alteration. Therefore, a choice was made to recreate conditions similar to those found in the field. The mock-ups were exposed to sunlight under ambient laboratory-controlled conditions. *Fresco* blocks were placed onto a windowsill at UCLA/Getty training laboratories at the Getty Villa in Malibu, CA, and exposed to sunlight for 10 weeks. Light levels, temperature, and relative humidity (RH) were recorded indicating variations within and across the days of exposure ranging between 0 and 4500 lux, 0–500 μW/lm, 23–36 °C, and 35 % ± 5 % RH. The setup avoided any outdoor exposure which could introduce uncontrolled contamination by atmospheric pollutants or weathering of the sample surfaces and subsequently add to the complexity of studies.

2.5 Preventive and remedial conservation: *protection from light and desalination*

Previous work has shown that cinnabar alteration is an irreversible process. Once the wall painting surface pigmented with cinnabar has blackened, it cannot be reconverted to its previous red state. Therefore, one of the objectives of this research focuses on determining what steps, if any, could be taken to inhibit, curtail, or slow down the alteration process of freshly excavated wall paintings painted with cinnabar. Two primary strategies are explored: [1] varying the moment of light exposure during the drying process and [2] chlorine ion reduction via desalination.

Accounts on cinnabar darkening [32, 49] have suggested that beside light exposure, moisture may also enhance or accelerate the rate of color change. In order to explore how varying the moment of light exposure during the drying process would impact the extent of alteration, specifically to check whether low moisture levels at the time of light exposure would retard the alteration, mock-ups were divided into two groups. *Group A* was exposed to light while wet; blocks were placed under direct sunlight immediately upon their removal from a salt solution. *Group B* was dried prior to light exposure; mock-ups were allowed to dry in the dark under ambient conditions until they came to a constant weight before they were exposed to light.

McCormak [27] noted that geological specimens of cinnabar with an average over 0.05 Cl wt% are photosensitive; those with an average below 0.01 Cl wt% are not photosensitive. To test this hypothesis, after the exposure of the blocks to saline solutions, chlorine ions were removed from the salt-contaminated *fresco* via a desalination process. The goal was to place the Cl wt% below this threshold prior to light exposure. Mock-ups were removed from the salt solution and allowed to partially dry in darkness under ambient conditions for 3 days. At the end of this period, samples were cool to the touch while continuing to loose weight. As most *fresco* paintings are often recovered from damp soil, they tend to have relatively high water content. Allowing samples to dry partially replicates this type of environment. Subsequently, samples were desalinated with cellulose poultices (Fig. 1). Cellulose fibers (Arbocel® BC 200) and deionized water were combined in a 1:5 ratio to form a paste. Subsequently, this paste was gently pressed against the surface of the block creating a 1-cm-thick compress. It should be noted that a permeable layer of thin Japanese tissue (MMN-1 Tengucho-Hiromi

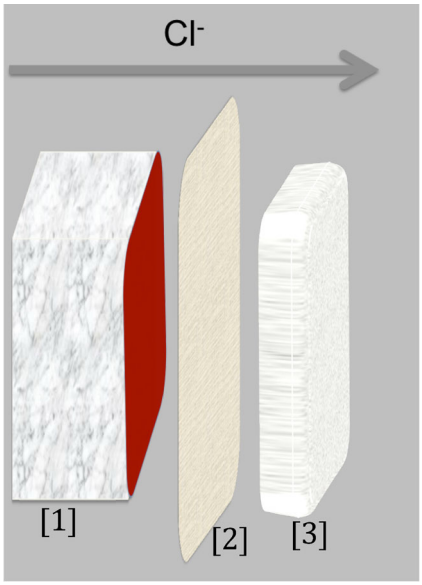

Fig. 1 Schematic representation of the desalination process. Fresco mock-ups [*1*] were desalinated (to remove the Cl^- ions) using cellulose fiber-based compresses [*3*]. A thin Japanese tissue (MMN-1 Tengucho-Hiromi) barrier layer [*2*] was placed between the mock-up and the poultice. Cellulose fibers and deionized water were combined in a 1:5 ratio to form a 1-cm-thick compress across the block [*3*]. As the cellulose fibers dried, Cl^- ions present within the block were drawn out of the block and into the poultice

paper: 5 g/m^2) was placed at the interface between the poultice and *fresco* mock-up to prevent cellulose fibers from adhering to the surface of block. Blocks were then allowed to stand until the cellulose fibers were dry to the touch (approximately 72 h). Poultice was then removed, and conductivity of rehydrated poultice was measured as an indication of the salt (NaCl) extracted. This process was repeated five times, after which mock-ups were exposed to light as described above.

2.6 Artificial accelerated weathering of pigment powders

As a point of comparison, samples of powdered pigment were also artificially weathered through the exposure to 0.1 and 5 M saline solutions (NaCl) and to the light. Cinnabar was combined with saline solution at a 1:25 w/v ratio, mixed thoroughly and allowed to stand for approximately 12 h in the dark. At the end of this period, the saline solution was decanted, and approximately 0.25 g of cinnabar was spread onto the surface of each glass slide. In order to disambiguate the impact of moisture on the alteration process, the RH (relative humidity) of the environment was controlled during the drying process. Samples were alternately housed in inert polypropylene containers with gel silica conditioned to 5, 50, or 70 % relative humidity (RH). Finally, samples were placed directly onto the windowsill the Getty Villa in Malibu, CA, for a period of 21 days. Light levels and temperatures during this period varied within and across the days, ranging between 0 and 4500 lux, 0–500 μW/lm and 23–36 °C.

2.7 Sample preparation

Stratigraphic polished cross sections were prepared by embedding samples in Bio-Plastic® polyester resin and hardener purchased from Aldon Corp, Avon, NY. It is important to note the absence of chlorine commonly found in the epoxy resins often employed in conservation, which would otherwise interfere with the ability to examine the role of chlorine in the alteration process which is the focus of this work. Upon hardening, samples were ground using Buehler silicon carbide grinding papers from 240 to 1200 grit. Cross sections were subsequently polished on a Leco® GP-25 polishing turntable using 6- and 1-μm diamond paste thinned with isopropanol on Buehler® MasterTex and appropriate polishing cloths. Isopropanol was employed as an alternative to water for grinding/polishing in an effort to limit the loss of any sodium chloride or mercury chloride salts.

2.8 Characterization methods

2.8.1 Optical microscopy

The extent of paint layer discoloration and pigment alteration was evaluated at first using optical microscopy (OM) including polarized light microscopy (PLM) and digital microscopy (DM). Changes to the bulk surface of the blocks were captured using Nikon D90 Digital SLR camera allowing for qualitative assessment of color changes within and between blocks during aging. Images were recorded with a color reference panel and color corrections were made, as necessary, using Adobe Photoshop to ensure the colorimetric fidelity of the image.

Digital microscopy provided higher-resolution imaging of mounted (as polished sections) and unmounted (small fragments without any preparation) samples. Both polarized light microscopy and digital microscopy allowed enhanced visualization of individual blackened particles. Photomicrographs were taken with an Olympus BX51 polarized light microscope and under a KEYENCE VHX-1000 digital microscope at 20×, 50×, 100×, and 200× magnifications.

2.8.2 Ultraviolet, visible light, near-infrared (UV/Vis/NIR) reflectance spectroscopy and colorimetry

Color measurements were taken using the FieldSpec3® 3 by Analytical Spectral Devices Inc (ASD), with high

spectral resolution (3 nm @ 700 nm and 10 nm @ 1400/2100 nm) and wide spectral range between 350 and 2500 nm, spot size 8 mm. Spectro-colorimetric measurement allowed quantification of incident and reflected radiation intensities, which roughly equates to human color perception [29, 50]. Change in color (ΔE^*) was calculated with the following formula (Eq. 1) defined in 1976 by the CIE (Commission Internationale de l'Eclairage):

$$\Delta E^* = \left[(\Delta L^*)^2 + (\Delta a^*)^2 + (\Delta b^*)^2\right]^{1/2} \quad (1)$$

where ΔL^* describes the change in luminance, Δa^* the change in green/red components, and Δb^* the change in blue/yellow components.

Samples were analyzed only in the areas which appeared visibly altered (one measurement/spot per sample).

2.8.3 X-ray fluorescence (XRF) spectroscopy

For elemental characterization, the Thermo Scientific Niton® XL3t Series GOLDD™ technology handheld portable XRF was used, with a silver anode and silicon drift detector. Readings were taken with an 8-mm-diameter spot size in both Soil Mode and Mining Mode for 120 s for each measurement. Result was an average of three measurements. This technique provided semiquantitative information regarding relative concentrations of chlorine in the cinnabar (HgS) pigment and unaltered samples.

2.8.4 Scanning electron microscopy (SEM) and energy-dispersive X-ray spectroscopy (EDS)

As the degradation layer is typically quite thin (several micrometers or less), scanning electron microscopy enabling high spatial resolution was used. Scanning electron microscopy (SEM) was performed with a FEI Nova™NanoSEM 230. To avoid the necessity of carbon or metal sputtering, a low vacuum mode (variable pressure) was applied during the analysis. Morphological characteristics of the surface and topographical contrast were recorded with the secondary electron detector (SE) using the low vacuum detector (LVD). Compositional contrast was assessed with the backscattered electron detector (BSE) using a gaseous analytical detector (GAD), and spatially resolved elemental analysis was performed with a Thermo Scientific NORAN System 7 energy-dispersive X-ray spectrometer (EDS).

Samples were first examined noninvasively at low vacuum, in order not to damage, dehydrate, or alter the materials. Polished cross sections were also analyzed with SEM–EDS for spatially resolved inter- and intra-layer visualization and characterization. Elemental spectra and maps of characteristic X-ray photon emissions were acquired using EDS. The analysis of well-polished surfaces was crucial for more precise quantitative measurements because of the shallow probing depth of electrons interacting with the surface. In addition, flat surfaces minimize the deflection of BSE in different directions, maximizing the collection of electrons by the detector located symmetrically to the incident beam of electrons. EDS spot analysis enabled comparisons of peak intensities, providing data regarding relative concentration of the chlorine (Cl) and sulfur (S) found in the specimen, and elemental mapping of certain areas provided a visual of the profile distribution of these elements.

2.8.5 Powder X-ray diffraction (XRD)

Powder X-ray diffraction (XRD) provided characterization of the crystal phases within the degradation products observed on the artificially weathered mock-ups. This technique served as a means to assess samples for the presence of new compounds, as well as conformational changes within the cinnabar molecule, specifically the occurrence of mercury chloride-containing salts or HgS polymorphs. For the analysis, to ensure that measurement is representative, a few particles of the area of interest were mounted on a glass spindle using Apiezon high vacuum grease and analyzed using a Rigaku R-Axis Spider X-ray diffractometer. XRD spectra were recorded at 50 kV/40 mA using a Cu-Kα target for 900 s. Bulk powder samples were run for 1200 s. XRD data were processed and matched against reference spectra from the International Center for Diffraction Data (ICDD) files using the JADE, v8.2 software from Materials Data Inc.

2.8.6 Thermodynamic modeling

Thermodynamic calculations were carried out at 25 °C and 1 bar using GEMS-PSI: Gibbs Energy Minimization Software package, version 2.0 [51]. GEMS is a broad-purpose geochemical modeling code which uses Gibbs energy minimization criterion and, in conjunction with information of the thermodynamic properties of phases (i.e., solids, liquid, and air), computes equilibrium phase assemblage and speciation in a complex chemical system from its total bulk elemental composition. Chemical interactions involving distinct solid phases, solid solutions, and the aqueous electrolyte(s) are considered simultaneously. Thermodynamic properties of solid and aqueous species were sourced from the GEMS-PSI standard database for minerals and amended with additional information relevant to mercury-containing phases. Input data for mercury-bearing solids (Table 1) were taken from Radepont [29].

Table 1 Free energies of formation of mercury-bearing phases considered in this study

Phase	ΔG_f^0 [kJ/mol]
Cinnabar (α-HgS)	−45.77
Meta-cinnabar (β-HgS)	−43.66
Calomel (Hg_2Cl_2)	−210.37
Mercuric chloride ($HgCl_2$)	−180.30
Corderoite (α-$Hg_3S_2Cl_2$)	−406.99
Metallic mercury; quicksilver (Hg(0))	0

Thermodynamic modeling was carried out to provide insight into pure cinnabar alteration in the presence of sodium chloride and when applied in the *fresco* technique. This is a generic equilibrium-based approach that does not take into consideration the impact of kinetic reactions or light that may significantly alter the phase assemblage found under real environmental conditions. However, it does serve as a useful guide for predicting phases, which are anticipated to be thermodynamically stable under particular conditions. Three possible scenarios were examined: [1] the bulk cinnabar pigment mineral; [2] pigment on a fully carbonated *fresco* surface; and [3] pigment on carbonated *fresco* surface which also contains a slight amount of $Ca(OH)_2$. Each of these systems was set to a 0.1 M NaCl solution and modeled as a function of increasing amount of the atmospheric air, which was progressively added to the system. The 5 M NaCl solution scenario was not simulated as current aqueous ion activity model implemented in GEMS can make reliable predictions for molar strengths only up to 2–3 M. Information regarding variations in the redox potentials (Eh) as well as pH of the aqueous solutions was recorded in order to assess their impact on phase formation.

3 Results

3.1 Discoloration of *fresco* wall painting mock-ups

The pH of the saline solutions was tested before and after infusion, with a Merck pH strip. Indicator strips dipped into the solution when the blocks were first placed into contact with saline solution showed a pH of 7; after 12 h in contact, the solution had a pH of 12.

Minor alteration was also observed on the surfaces of control block (Fig. 2a[I–VIII]). Those placed into the light with no treatment or having been wet only with DI H_2O exhibited a fine gray haze covering much of the surface (Fig. 2b[I–VIII]). This is likely the result of trace amounts of chlorine within the $Ca(OH)_2$ (lime putty) used to fabricate the test blocks. XRF analysis of the surface of the blocks prior to accelerated artificial weathering using saline solutions found an average of 0.03 Cl wt% in each. Photographs and color measurements taken of the simulated *fresco* blocks pigmented with cinnabar and infused with saline (NaCl) solution over the 10-week period of light exposure captured the swift and dramatic discoloration of red cinnabar into gray/black (Fig. 2c[I–VIII]–f[I–VIII]). In the presence of 0.1 M of NaCl, the color change in the surface was visible within the first 6 h of light exposure both when dried in the light and when dried in the dark (and then exposed to light) (Fig. 2c[I–VIII], e[I–VIII]). Similar patterns were observed also for the blocks infused with 5 M NaCl (Fig. 2d[I–VIII], f[I–VIII]). Generally, it appears that the alteration began at the edges of the samples and progressed inwards. After 70 days, the *fresco* simulated blocks which were in contact with chlorine solution (Fig. 2c–f), showed significant discoloration; the previously bright red surface became muted and mottled (Fig. 2c[I–VIII]–f[I–VIII]). A light lilac-gray alteration was visible in select areas across the surface, and the edges were a deep gray/black. The color values of these transformations are shown in Table 2. It was noted that color change that occurred on the surface has increased with molarity of the solution; blocks impregnated 5 M solutions (Fig. 2d, f) show more significant change in color (Table 2: blocks D and F) as compared to 0.1 M solution (Fig. 2c, e; Table 2: blocks C and E). However, it was also observed that both color and surface morphology of blocks wet with a 5 M NaCl solution were impacted by the formation of white halite crystals (Fig. 2d[I–VIII], f[I–VIII]).

Microscopic optical examination of cross sections from darkened areas shows that, while the color change observed is intense, the alteration is highly superficial; it only occurs at the surface and subsurface ranging from 5 to 20 μm in depth (Fig. 3). Examination of the surface cross section at high magnifications suggests that variation in color observed at the macroscopic level is a product of both the extent to which an individual particle has altered and the density of altered particles. Blackening of individual particles begins along the edges and moves inwards with total color discoloration of the smaller particles (Fig. 4). The overlay of a fine black degradation layer across the intact red substrate causes the particle to appear a deep maroon. The relative proportion of red to black particles has a similar effect (Fig. 5). In areas with a high concentration of black particles, the surface appeared more gray–black (Fig. 5c), whereas in areas with a greater mixture of red and black particles, the surface takes on a hazy grayish–purple (Fig. 5d).

3.2 Discoloration of pigment powders

Examination of the powder samples of cinnabar showed similar results (Table 3). Only the cinnabar powders

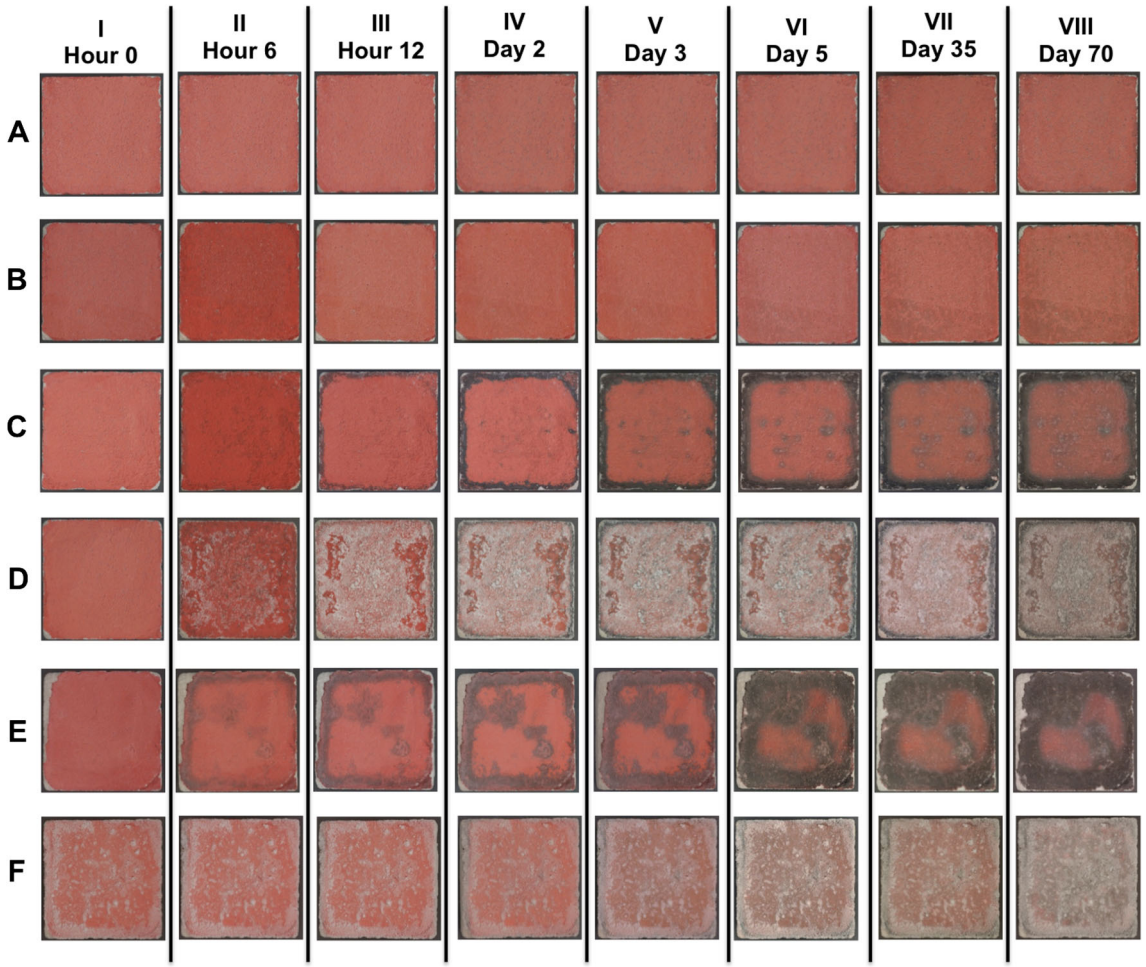

Fig. 2 Images of the surface of fresco wall painting mock-up blocks captured during a 10-week period (70 days) of light exposure on a windowsill at the Getty Villa in Malibu, CA, at RH ~35 %. The blocks were infused (via capillary action) with saline solution in order to induce alteration of the surface upon subsequent light exposure with the exception of **a**[*I–VIII*] and **b**[*I–VIII*] that act as control samples. **a**[*I–VIII*]: No exposure to any solution prior to placement in light; **b**[*I–VIII*]: Exposed to DI H_2O alone, dried in the light; **c**[*I–VIII*]: Exposed to 0.1 M NaCl solution, dried in light; **d**[*I–VIII*]: Exposed to 5 M NaCl solution, dried in light, **e**[*I–VIII*]: Exposed to 0.1 M NaCl solution, dried in dark prior to placement into light exposure; **f**[*I–VIII*]: Exposed to 5 M NaCl solution, dried in dark prior to light exposure. Images were taken at different time intervals: *I* = Hour 0; *II* = Hour 6, *III* = Hour 12, *IV* = Day 2; *V* = Day 3; *VI* = Day 5; *VII* = Day 35; and *VIII* = Day 70. *Note* Images in lines B, C, and D column II after 6 h were still wet so the color of the blocks appears more saturated; by 12 h, they had dried, and the color now appears more muted and is consistent with the *color* of the other *dry blocks*

Table 2 Color change in bocks over 70 days of light exposure captured with UV/Vis/NIR spectrometer

Block	Pre-experiment values			Value after 70-day aging			Change in color ΔE^*
	L^*	a^*	b^*	L^*	a^*	b^*	
A	66.72	27.97	16.183	63.85	24.89	12.77	5.40
B	62.43	28.99	15.84	61.35	26.68	14.44	2.98
C	60.61	30.81	18.73	61.48	25.13	13.31	7.90
D	62.27	29.81	18.34	73.55	6.90	0.90	30.93
E	69.68	9.15	14.18	76.71	3.10	0.86	7.21
F	66.63	26.03	15.14	74.43	3.37	0.92	27.87

Block designations A–F refer image displayed in Fig. 2

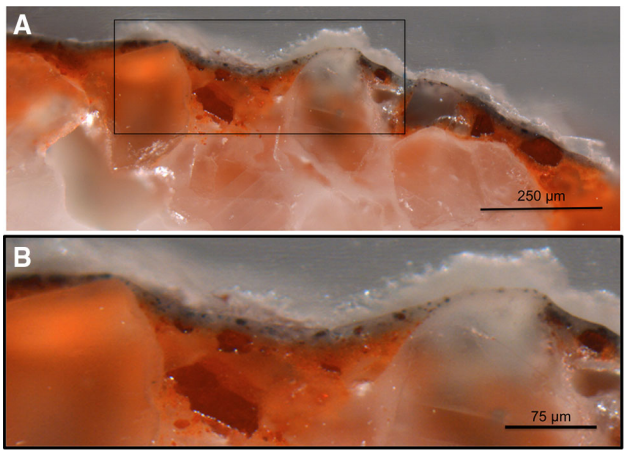

Fig. 3 Cross section removed from a blackened area of fresco block impregnated with 5 M NaCl solution, dried in dark, and subsequently exposed to light for 70 days. **a** The fresco is comprised of four discrete layers; [1] the white $CaCO_3$ fresco substrate prepared by combining $Ca(OH)_2$ with marble dust aggregate, [2] *red* HgS pigment, [3] altered/blackened particles, and [4] surface crust of halite crystals. **b** Examination in cross section shows the alteration layer to be highly superficial; it only occurs at the surface and subsurface of approximately 5–20 µm depth

exposed to saline solution, light, and relatively high RH (between 50 and 75 %) showed evident color change from red to black. Cinnabar treated with DI H_2O remained red regardless of light exposure, and cinnabar kept in the dark remained red regardless of exposure to saline solutions. Cinnabar powders exposed to 0.1 M saline solutions, light, and RH between 50 and 75 % (Fig. 6c[I–IV]) as well as those exposed to 5 M NaCl solution, light, and RH at ~50 % (Fig. 6d[I–IV]), showed severe blackening. The pattern of alteration in the 0.1 M NaCl is uniform and spreads homogeneously over the entire surface of the particles. In the 5 M NaCl, the blackening is speckled with spots of intense blackening surrounding the halite (NaCl) crystals. The artificially weathered samples (exposed to saline solutions) and placed in a low RH environment (~5 %) showed no color change over the 21-day period of light exposure (Fig. 6a[I–IV]). In contrast, those exposed to a high RH environment (~50–75 %) and light demonstrated intense and significant blackening Fig. 6c[I–IV], d[I–IV]).

3.3 Change in morphology and chemical change

High-resolution SEM imaging of the darkened particles indicated a change in their morphology; the black particles display a distinct amorphization when compared to the characteristic rhombohedral/tabular habit of the red control particles (Fig. 7a, c). Figure 7b, d, shows the change in the particles morphology after exposure to 0.1 M NaCl solution and light.

EDS spot analysis and elemental mapping of cross sections showed the presence of Na, Cl, Hg, and S within both the altered and unaltered areas. Despite extensive investigations, no correlation could be made between the presence of chlorine and the color of the particle. Chlorine was present both in the red and black particles and was always found in association with sodium (Fig. 8). The elemental concentrations and distribution (Fig. 8c) suggested the presence of a sodium chloride phase rather than a mercury chloride-containing compound. However, a qualitative reduction of sulfur in the blackened particles was observed (Fig. 8c—see map of S in the black particle). Standardless EDS analysis on the red and black particles in the powder samples confirmed lower sulfur to mercury ratio in the black particles (Fig. 9; Table 4) and an

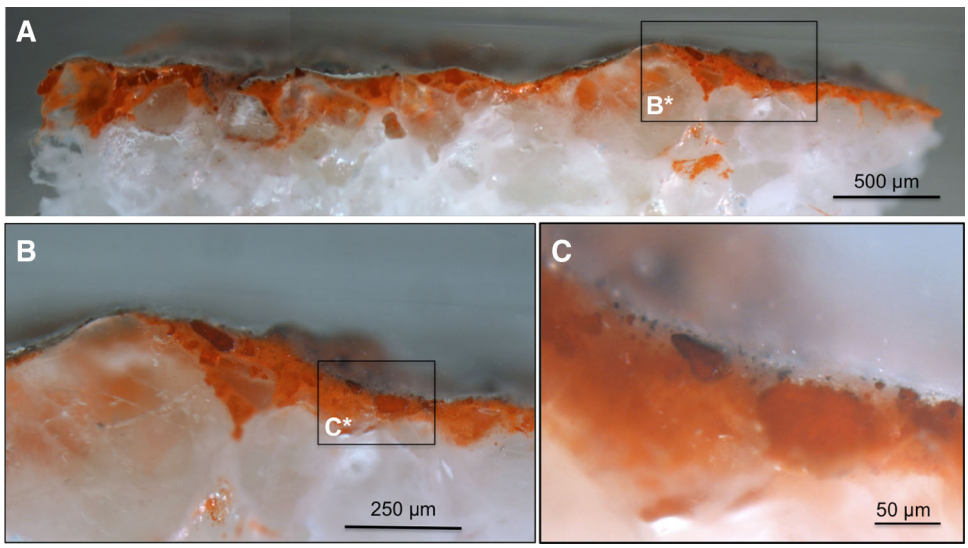

Fig. 4 **a** Cross section removed from blacked section of fresco block impregnated 0.1 M NaCl solution and exposed to light for 70 days. **b** Very thin alteration layer; the particles at the surface has just begun to blacken. **c** Highly magnified image of the altered surface shows that blackening of individual particles begins along the edges

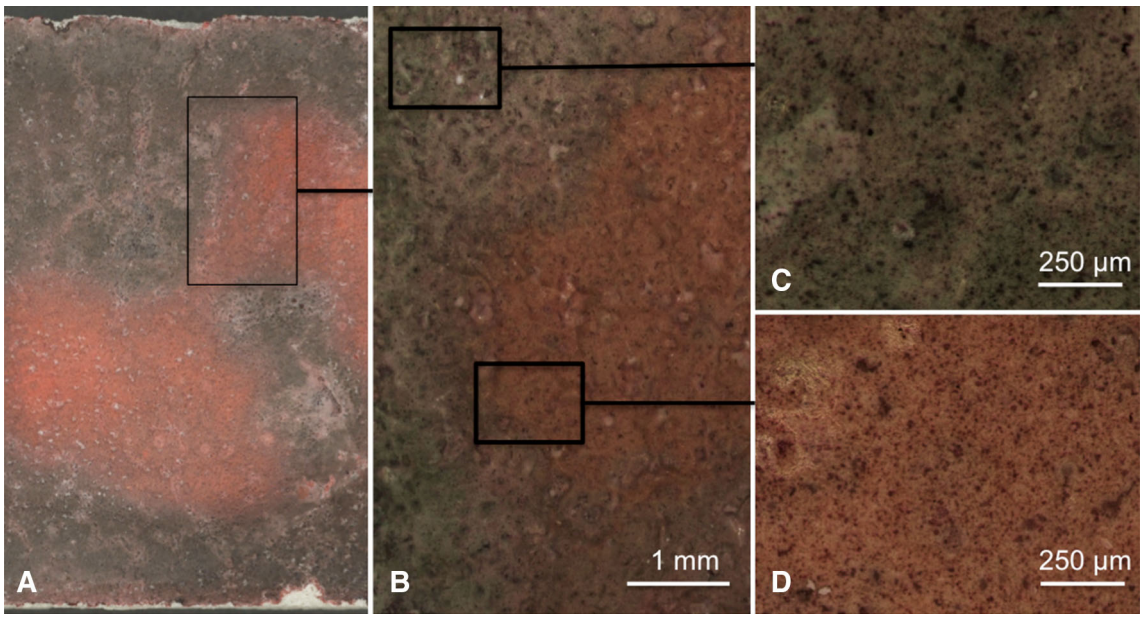

Fig. 5 **a** Central part of a fresco block impregnated in 0.1 M NaCl solution, dried in the dark, and subsequently exposed to light for 70 days. The photograph shows the variation in color observed when examining the alteration layer at the macroscopic level; the surface ranges from a *dark pink* to a *soft purple–gray* to a *deep gray–black*. **b** Magnified image of altered surface. Microscopic examination reveals that the color change relates to the intensity of relative proportion of red to *black particles*. **c** Areas with a high concentration of black particles on the surface appeared *gray–black*. **d** Areas with a greater mixture of red and black particles on the surface take on a hazy grayish–purple

Table 3 Presence or absence of alteration observed in cinnabar powders upon exposure to DI H_2O, 0.1 M NaCl solution, or 5 M NaCl solution as impacted by light exposure and relative humidity (italic cells displayed color change)

Solution salinity	RH (±5 %)	Light exposure	Visible alteration
DI H_2O	5	No	No
DI H_2O	5	Yes	No
DI H_2O	50	No	No
DI H_2O	50	Yes	No
DI H_2O	75	No	No
DI H_2O	75	Yes	No
0.1 M	5	No	No
0.1 M	5	Yes	No
0.1 M	50	No	No
0.1 M	*50*	*Yes*	*Yes*
0.1 M	75	No	No
0.1 M	*75*	*Yes*	*Yes*
5 M	50	No	No
5 M	*50*	*Yes*	*Yes*

enrichment in chlorine. The ratio of sulfur to mercury in the unadulterated particles is close to 1, whereas the altered areas show an average ratio of 0.9. This indicates a depletion of sulfur in the blackened particles.

SEM–EDS analysis of a sample taken from the surface of the *fresco* before the infusion of 0.1 M NaCl solution or exposure to light showed a veil of rhombohedral calcium carbonate crystals across the surface of block characteristic of the carbonation process of calcium hydroxide occurring in a *fresco* application (Fig. 10a). Analysis of an area of blackened surface, after the introduction of the saline solution and light exposure, indicates a change in the appearance and elemental composition. The altered areas show precipitation of thin films of the unknown phase which have ~10–15 µm in diameter (Fig. 10b) and are partially covering the calcium carbonate crystals. EDS spot analysis of selected altered areas (Fig. 10d) indicated a heightened presence of calcium and sulfur on their surface which may be indicative of gypsum formation ($CaSO_4 \cdot 2H_2O$). The presence of calcium, oxygen, and carbon was detected on both altered and unaltered samples (Fig. 10c, d), but sulfur was found to be present on the altered surfaces within the "Islands."

No Hg was detected as cinnabar particles are present below the particles of $CaCO_3$ (calcite) that formed on the top of the surface as a result of atmospheric carbonation of $Ca(OH)_2$ plaster. As such, HgS particles are "locked" underneath the $CaCO_3$, and since EDS analysis has a spatial resolution of around 1 µm, HgS identification was hindered. Lack of Hg and presence of S on the altered surfaces may suggest that after HgS was decomposed,

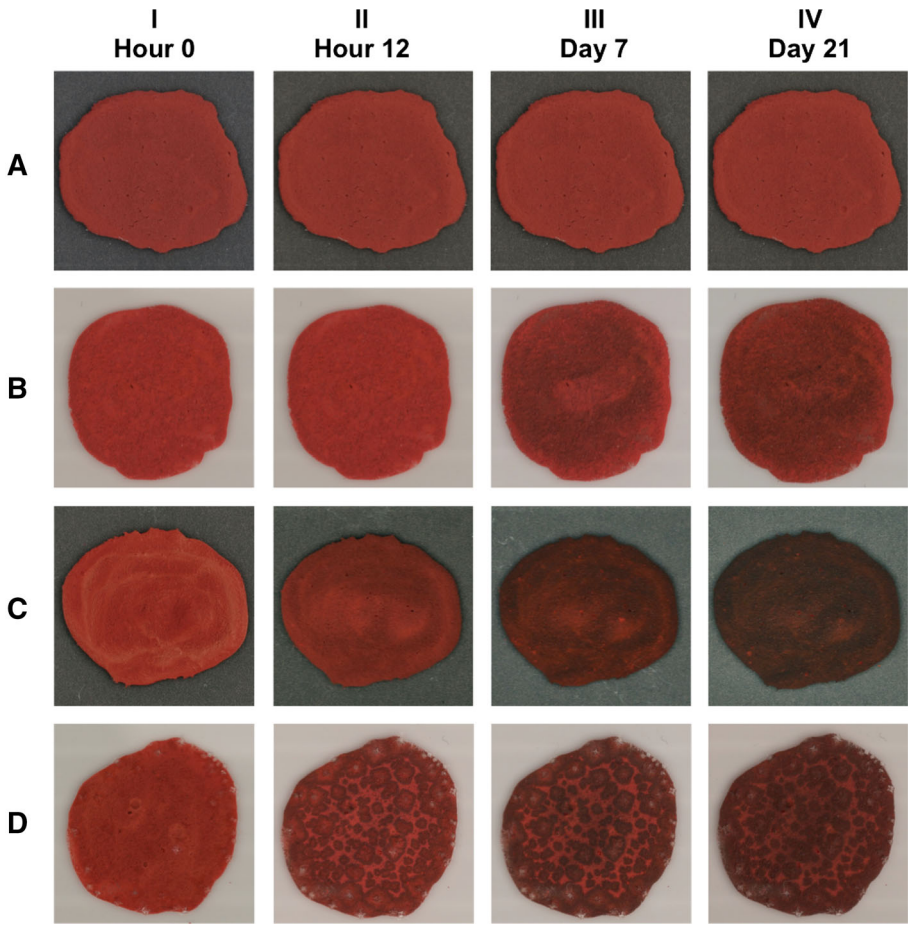

Fig. 6 Images of bulk cinnabar powder captured during the 21-day period of light exposure in a windowsill at the Getty Villa in Malibu, CA. **a**[*I–IV*]: Exposed to 0.1 M NaCl solution and kept at 5 % RH; **b**[*I–IV*]: Exposed to 0.1 M NaCl solution and kept at 50 % RH; **c**[*I–IV*]: Exposed to 0.1 M NaCl solution and kept at 70 % RH; **d**[*I–IV*]: Exposed to 5 M NaCl solution and kept at 50 % RH: note small spots of halite crystals forming on the surface

sulfur (S) migrated toward the surface and reacted with calcium (Ca), while mercury (Hg) remained underneath the $CaCO_3$ film and hence was not detected through the EDS analysis.

3.4 Compound identification

XRD analysis of all samples recovered from the *fresco* blocks infused with NaCl showed consistent results. Cinnabar, calcite, and halite were identified in all samples, and calomel was detected in most (Table 5; Figs. 11, 12). These results are significant as they suggest that the formation of calomel appears to be independent of (1) exposure to light and (2) color of the sample. When blocks were dried in the dark and subsequently exposed to light, calomel was still detected in both, before and after light exposure. Calomel was present in visually unaltered, as well as altered, areas of the block; it was detected on both red and black areas of the samples, suggesting that it is not directly responsible for the observed color change in the samples.

3.5 Desalination

As already mentioned above, minor alterations were observed on the control samples exposed light (Fig. 2a, b) which is likely linked to the small quantities of chlorine within the lime putty used to produce test blocks. XRF analysis of the surface of the blocks prior any exposure to saline solutions found an average of 0.03 Cl wt% in the samples.

Attempts to inhibit or retard the alteration process through desalination using successive compresses of deionized water (DI H_2O) were found to be relatively unsuccessful, though very informative. The surfaces of blocks desalinated exhibited similar or sometimes even enhanced discoloration (5 M NaCl cases) upon light exposure when compared to samples which were not desalinated (Fig. 13). However, it was noted that in case of blocks treated with 0.1 M NaCl solutions, desalinated samples (Fig. 13d) appeared slightly less altered (especially center of the sample) as compared to the ones which were not desalinated (Fig. 13a). In case of 5 M NaCl-

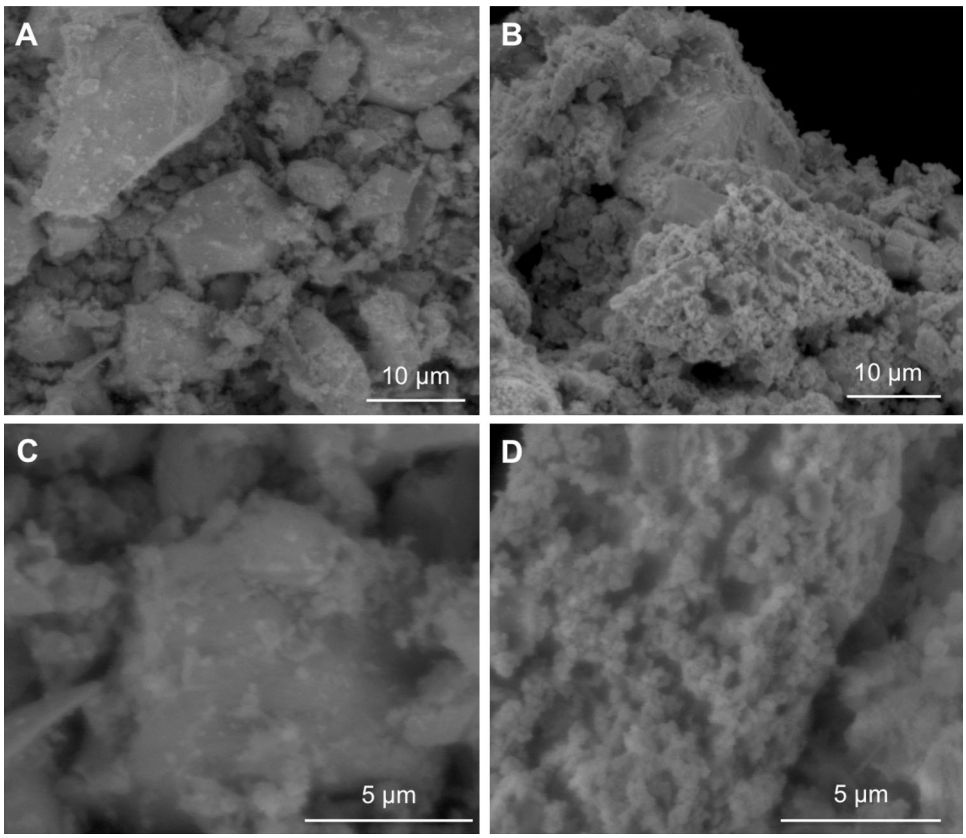

Fig. 7 Secondary electron micrographs at variable pressure of cinnabar powder samples. Images **a** and **c** show control red particles, those that had been exposed to neither saline solution nor light, which exhibits the characteristic rhombohedral/tabular habit of cinnabar. Images **b** and **d** show blackened cinnabar particles, those exposed to 0.1 M NaCl solution and exposed to light over 21 days, exhibiting more granular morphology

treated blocks, samples which were desalinated turned out black (Fig. 13e) upon the prolonged exposure to light, while samples which were not subjected to desalination looked gray (Fig. 13b). This gray appearance is associated with precipitation of white crystals on the surface of *fresco* blocks. These crystals were analyzed by XRD and identified to be halite (NaCl). Their potential impact on the darkening process is explained in the discussion section.

3.6 Thermodynamic modeling predictions

Figures 14, 15, and 16 demonstrate "progressive equilibrium approach" showing changes in phase assemblages as a function of increasing amount of air (oxygen activity) and resulting redox potential. To represent different scenarios, three mineral systems which are in contact with 0.1 M NaCl solutions were considered in this study: pure α-HgS pigment (Fig. 14), α-HgS + $CaCO_3$ which is the primary binder in wall paintings (Fig. 15), and α-HgS + $CaCO_3$ + slight amount of $Ca(OH)_2$ to show how a small quantity of uncarbonated binder may affect pH and therefore phase composition (Fig. 15). The formation of cinnabar (α-HgS), corderoite (α-$Hg_3S_2Cl_2$), calomel (Hg_2Cl_2), and metallic mercury (Hg(0)) was predicted in all three scenarios. Potential for the formation of all these phases has been also recently demonstrated by Radepont et al. [37]. It was noticed that the presence of calcium carbonate (Fig. 15) or calcium hydroxide (Fig. 16) significantly affected predicted phase assemblages when compared to the pure cinnabar pigment (Fig. 14). The amount of atmospheric air, which was put in contact with the input compositions, has also greatly influenced redox potentials and the pH of the simulated systems. Radepont et al. [37] have shown that redox potentials and fluctuations in oxygen activity can significantly affect phase equilibria. However, in their study to recreate changes in redox conditions, they have used sodium hypochlorite (NaOCl), a highly oxidizing agent. This research differs in that it replicates more realistic conditions that are encountered in real case scenarios involving archaeological wall paintings, which is the focus of this paper and therefore models systems with NaCl solutions (a common salt found in most archaeological sites) at different aerobic environments. The proposed model allowed to recreate a range of redox environments, while taking into consideration not only cinnabar as a pigment but also the chemical nature of the wall painting itself.

Changes in the solid phases, which are predicted to precipitate, were directly linked to changes in the aqueous phase such as pH or the variations in the redox potential of the system. Despite its inclusion in the model, mercuric chloride ($HgCl_2$) was never predicted to precipitate for the conditions computed in this study. Meta-cinnabar (β-HgS)

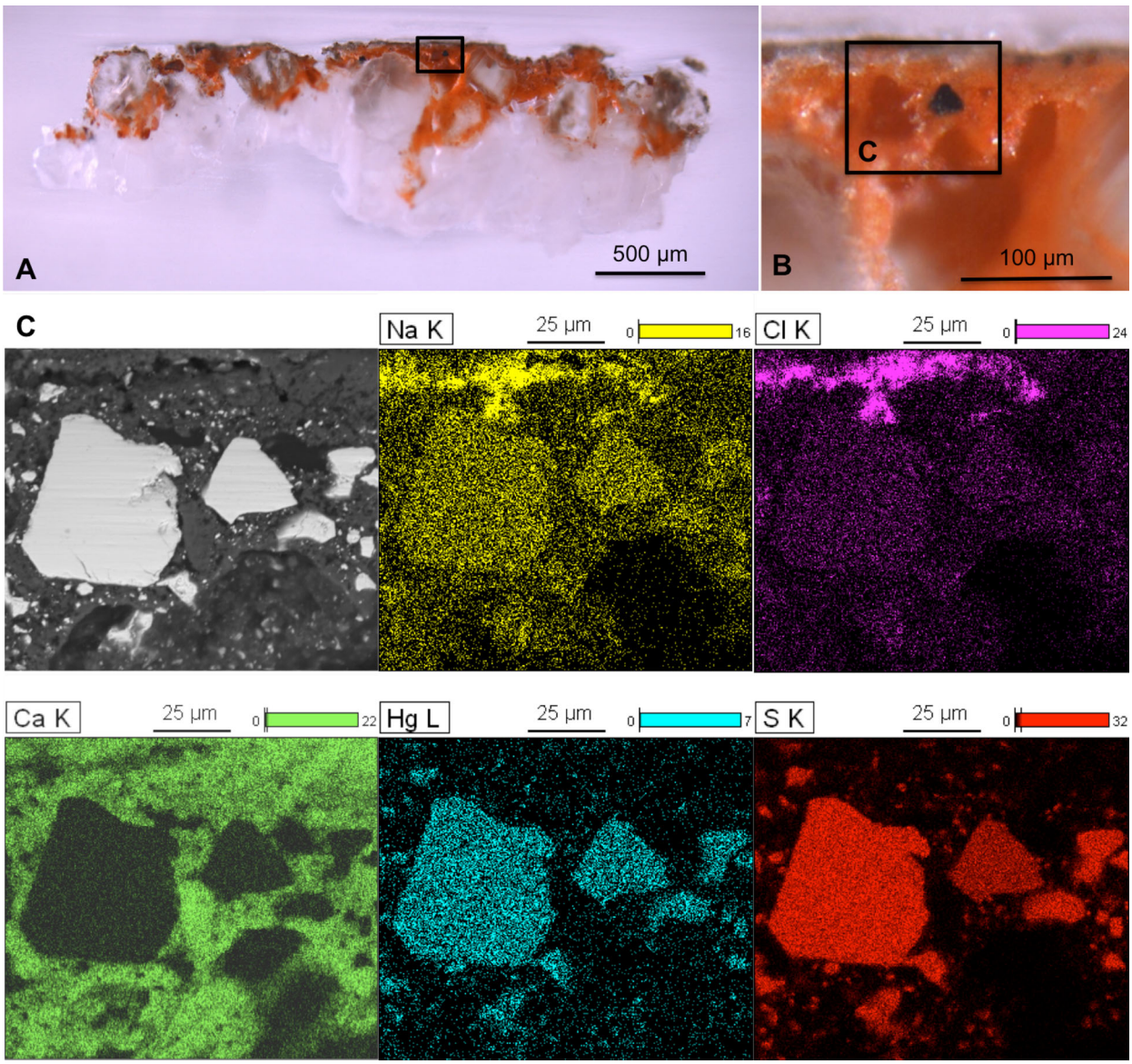

Fig. 8 **a** Cross section removed from a blackened area of the surface of a *fresco* mock-up block impregnated in 0.1 M NaCl solution, dried in the dark, and subsequently exposed to light for 70 days. **b** Detail of the black and red particles in **a**. **c** BSE image and elemental maps indicating the spatial distribution of sodium, chlorine, calcium, mercury, and sulfur within the red and black particles pictured in **b**

was also not anticipated to form under any of the scenarios simulated in this work (25 °C and 1 bar pressure). The occurrence of corderoite (α-$Hg_3S_2Cl_2$) appears largely unaffected by the redox potential of the environment but was significantly impacted by changes in the pH; it only occurred when the pH of the aqueous solution was below 8, which confirms earlier findings that extremely acidic conditions are not necessarily needed to favor the formation of this phase [37]. However, contrary to Redepont et al. [37], above pH 8, corderoite formation was not observed (Figs. 15, 16). As a result, the formation of corderoite was significantly limited in the presence of calcium hydroxide ($Ca(OH)_2$), which elevated the pH of the system. Formation of metallic mercury (Hg(0)) was favored under reducing conditions and in a wide pH ranges. However, elevated pH, e.g., by the presence of calcium hydroxide ($Ca(OH)_2$), seemed to significantly favor the formation of metallic mercury even under oxidizing conditions (Fig. 16). The precipitation of calomel appears to require oxidizing conditions (Figs. 14, 15, 16). As the amount of air which is put in contact with the material increases, the activity of O_2(g) will be elevated. The redox potential will therefore increase, thus favoring the formation of calomel (Hg_2Cl_2) instead of corderoite (α-$Hg_3S_2Cl_2$). This observation is in agreement with findings reported in the literature [29]. It was additionally observed that for certain

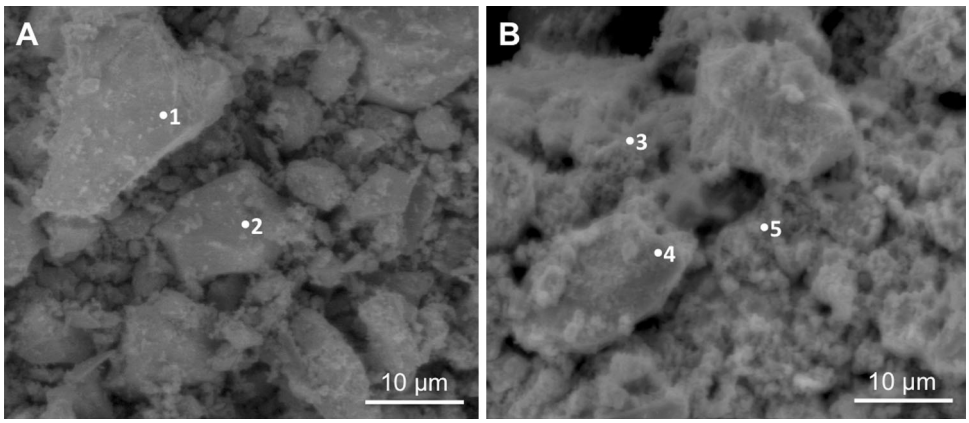

Fig. 9 SEM images taken at ×2000 magnification of bulk cinnabar particles; micrographs were recorded with the secondary electron detector (SE) using the low vacuum detector (LVD). Image **a** shows control *red particles*, those that had been exposed to neither saline solution nor light. Image **b** shows blackened cinnabar particles, those exposed to 0.1 M NaCl solution and exposed to light for over 21 days. Points *1–5* indicate areas analyzed using EDS (Table 5)

Table 4 Atomic % of elements measured on red unchanged (1 and 2) and black/altered (3, 4, and 5) cinnabar powder particles

Spot	O–Kα	Na–Kα	S–Kα	Cl–Kα	Hg–Lα
1	–	–	52.16 ± 2.20	–	47.84 ± 2.24
2	–	–	49.87 ± 3.02	–	50.13 ± 2.77
3	9.92 ± 0.96	–	37.23 ± 1.36	1.15 ± 0.16	51.71 ± 1.39
4	12.06 ± 1.01	1.13 ± 0.18	40.18 ± 0.71	1.60 ± 0.14	44.50 ± 1.15
5	17.64 ± 1.04	5.89 ± 0.34	32.18 ± 1.27	3.68 ± 0.32	40.61 ± 1.11

EDS analysis was carried out at 20-keV beam energy

oxidizing conditions when the pH is above 8 (Figs. 15, 16), gypsum ($CaSO_4{\cdot}2H_2O$) could be formed. This finding suggests that under certain circumstances, gypsum may form in a cinnabar system without the "necessity" of SO_2 species being supplied from an outdoor environment. Modeled scenarios indicate that transformation process of the cinnabar pigment is not straight forward and can be highly dependent on the nature of the system such as the amount of air in contact (and resulting redox potential), pH, or the presence of accompanying phases such as $CaCO_3$ and $Ca(OH)_2$.

Though $HgCl_2$ was included in the thermodynamic considerations, it was not predicted to precipitate under the conditions explored in this work. It has been shown that $HgCl_2$ can form directly via oxidation of Hg_2Cl_2 [37] above the redox potential (Eh) of 0.6 which is much higher than the one analyzed in this study.

4 Discussion

4.1 Conditions inducing the alteration

The work presented here confirms previous hypotheses that light and chlorine are dominant factors in the darkening of cinnabar. This study has further indicated that high relative humidity also plays an essential role in the transformation processes. Chlorine ions, light, and humidity were critical to inducing significant alteration in the HgS-pigmented *fresco* blocks and powder pigments.

Minor alterations were observed on the control samples exposed to light. This is likely the result of trace amounts of chlorine within the $Ca(OH)_2$ used to fabricate the test blocks. XRF analysis of the surface of the blocks prior to accelerated artificial weathering using saline solutions found an average of 0.03 Cl wt% in each. While this amount is just below the 0.05 Cl wt% threshold known to induce the alteration [27], it appears adequate to provoke localized subtle darkening of the surface. The attribution of this darkening to chlorine in concert with light, rather than light alone is supported by the results of laboratory trials involving powder cinnabar. Pure cinnabar powder exposed only to deionized water and placed under direct sunlight in ambient conditions showed no evidence of blackening after 21 days of light exposure, while significant changes were observed in pigment powders exposed to 0.1 and 5 M NaCl solutions.

The progression of blackening of the *fresco* mock-up blocks from the outer edges inward can likely be linked to heightened chloride content of those areas. During drying,

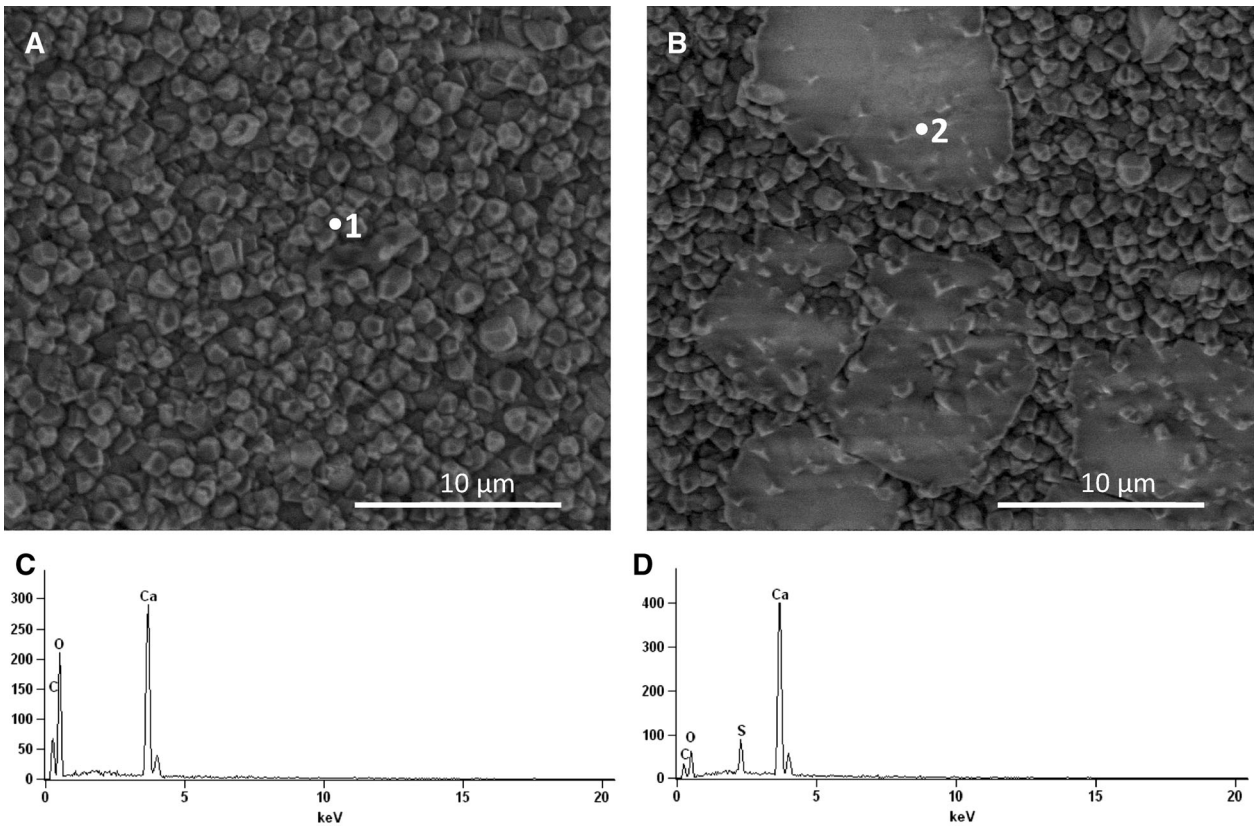

Fig. 10 SE micrographs (**a**, **b**) and EDS spectra (**c**, **d**) of control and altered blocks. **a** SE micrograph of the surface of the wall painting replica showing the calcium carbonate particles resulting from the carbonation of the calcium hydroxide binder in the plaster. **b** SE micrograph of the blackened fresco showing films of 10–15 µm diameter over the calcium carbonate crystals. Sample in image **b** was infused with 0.1 M NaCl solution, dried in the *dark* and subsequently exposed to *light* for 70 days. **c** and **d** show EDS spectra taken from point 1 (image **a**) and point 2 (image **b**) from the control and blackened areas, respectively

Table 5 Compounds identified on blocks in red and black areas both before and after light exposure (70 days)

NaCl solution (M)	Exposed to light	Sample color	Compounds detected			
			α-HgS	$CaCO_3$	NaCl	Hg_2Cl_2
0.1	Yes	Red	✔	✔	✔	✔
0.1	Yes	Black	✔	✔	✔	✔
0.1	No	Red	✔	✔	✔	✔
5	No	Red	✔	✔	✔	✔
5	Yes	Black	✔	✔	✔	–

highly concentrated NaCl solution formed along the sides. Air circulation at the rougher, more porous edges allowed for the enhanced evaporation over the smoothed, pigmented surface, creating localized areas with high concentration of chloride ions. Upon drying, the thickest halite crusts were found along the sides of each block. Interestingly, the correlation between increased Cl^- concentration and enhanced blackening was noted when comparing alteration on pigment powder samples treated with 0.1 and 5 M NaCl solution (Fig. 6), but it was more challenging to assess it in the case of mock-up blocks (Fig. 2). While pigment powders treated with 5 M NaCl solutions darkened more swiftly and pervasively than those treated with 0.1 M NaCl, the rate/degree of darkening of the mock-up blocks treated with 5 and 0.1 M NaCl was more difficult to evaluate. The lack of profound enhanced blackening on mock-up blocks treated with 5 M solutions is believed to be attributed to the layer of halite which had formed over the surface of 5 M NaCl-treated blocks. The halite crystals could have interfered with the reliable evaluation of the level of darkening in two ways: [1] by partially filtering/blocking the light and [2] by hindering blackening reaction

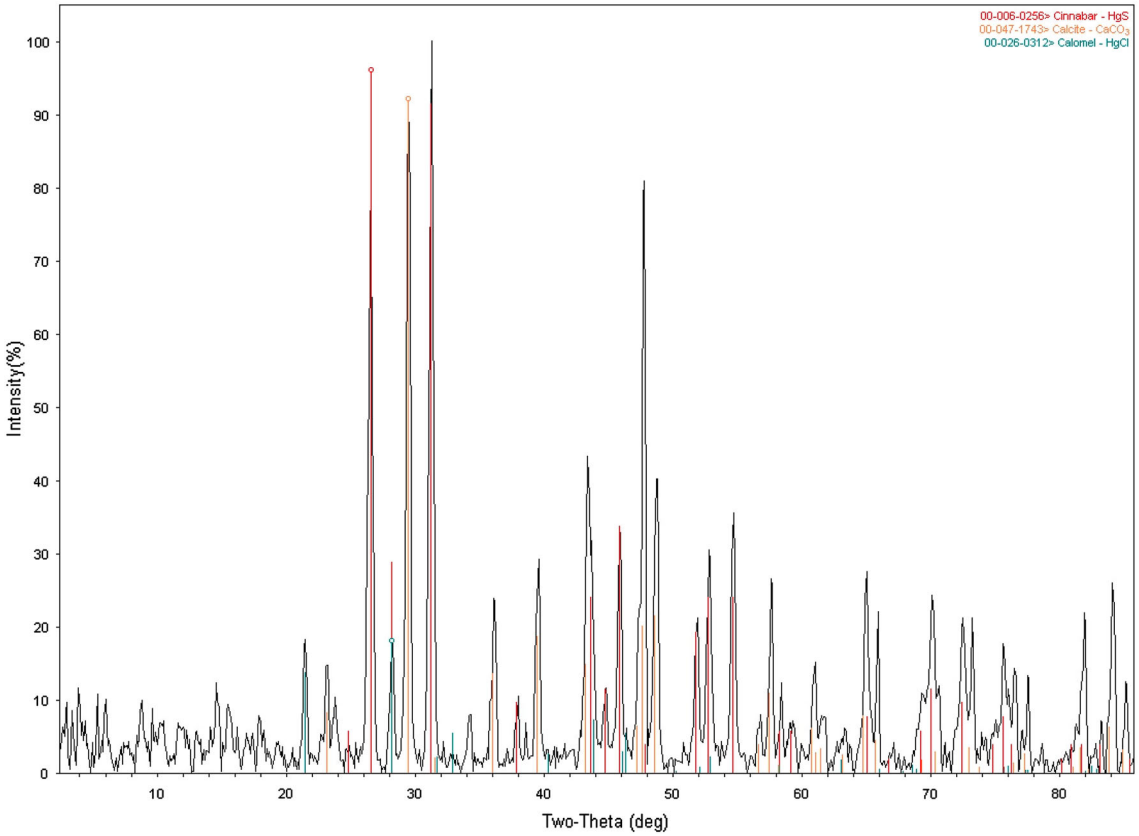

Fig. 11 XRD diffractogram of a *red area* sampled from a mock-up block infused with 0.1 M NaCl solution, dried in *dark* and then exposed to *light*. The diffractogram shows the major phases identified that include cinnabar, calcite, and calomel

due the hygroscopic nature of NaCl which acting as a desiccant absorbed moisture, that as shown in this study is an essential factor for the alteration of cinnabar.

Identification of the specific wavelength(s) of electromagnetic radiation that favor/provoke this alteration was beyond the scope of this study. It is notable, however, that during experiments carried out by Radepont et al. [36], cinnabar pellets exposed to NaCl solutions under UV irradiation required >120 days for the surface to show color change as compared to 6 h in the trials here. While differences in the experimental procedures prevent direct comparison, the disparity is dramatic and may indicate that visible, as well as ultra violet, wavelength plays an important role in the alteration process.

It was observed that the formation of halite crystals is dependent on the relative humidity (RH). For example when comparing the results of the fresco blocks (Fig. 2d) versus powdered samples (Fig. 6d) treated with 5 M solutions, it was found that halite crystals on the blocks were more profound. It is suspected that these crystals are not as visible in case of powdered samples as compared to blocks because these powdered samples were kept in higher relative humidity of 50 % RH versus blocks which were stored at 35 % RH. As NaCl is a deliquescent substance, it is dependent on the RH so higher RH could cause more NaCl to dissolve, and as a result, less halite crystals being present on the surface of powdered samples.

4.2 Alteration products and possible causes of darkening

4.2.1 Mercury chloride-containing compounds

XRD analysis detected the presence of a single mercury chloride compound. Calomel was identified on the surface of *fresco* samples exposed to saline solution, both before and after exposure to light. The formation of calomel in samples prior to light exposure is significant to understand the possible causes of color alteration in cinnabar and stands in opposition to previous reaction mechanisms proposed to explain the pigment's color change. While thermodynamic modeling of an HgS, NaCl, and H_2O containing system predicted the formation of calomel under certain conditions (Figs. 14, 15, 16), the reaction mechanism previously proposed by scholars largely suggests that calomel is formed as part of a secondary or

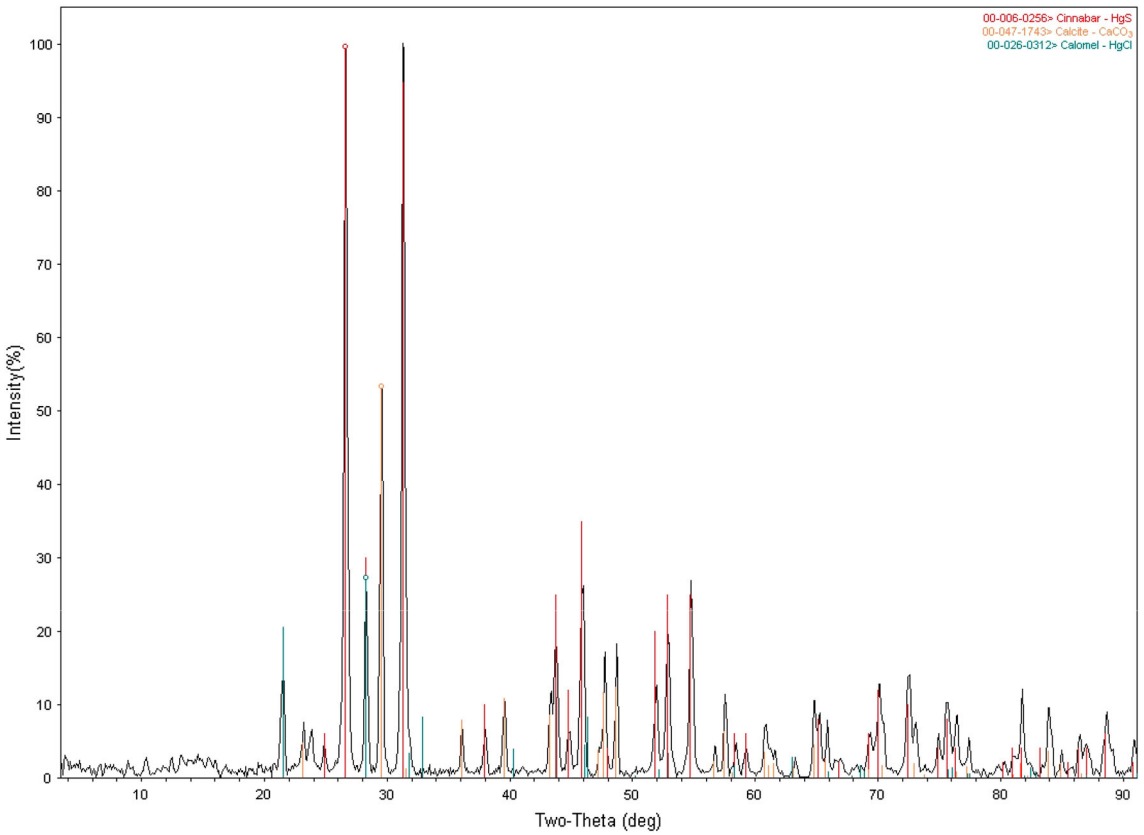

Fig. 12 XRD diffractogram of a *black area* sampled from a mock-up block infused with 0.1 M NaCl solution, dried in *dark* and exposed to *light*. The diffractogram shows the major phases identified that include cinnabar, calcite, and calomel; low intensity of some of the calomel peaks is believed to be associated with the preferred orientation effects

tertiary step, often after exposure to light. Keune and Boon [34] proposed that chlorine serves as a catalyst of photochemical redox reaction of Hg(II)S into elemental Hg(0) and S(0). Subsequently, Cl^- and Hg(0) react to form $HgCl_2$ and HgS to form corderoite ($Hg_3S_2Cl_2$) and S(0). Upon exposure to light, the photosensitive corderoite degrades into calomel (Hg_2Cl_2). This is followed by the light-induced disproportionation of calomel into Hg(0) and mercury(II) chloride ($HgCl_2$) (Eq. 2).

$$Hg_2Cl_2 \rightarrow HgCl_2 + Hg \quad (2)$$

Spring and Grout [23] also support that in the presence of light, corderoite degrades to form calomel, as well as sulfur and meta-cinnabar (β-HgS) as shown in Eq. 3.

$$\alpha\text{-}Hg_3S_2Cl_2 \rightarrow Hg_2Cl_2 + S + \beta\text{-}HgS \quad (3)$$

Radepont et al. [36] on the other hand suggested that cinnabar (α-HgS) is transformed to calomel via mercury sulfochloride intermediates (Eq. 4); however, unlike Keune and Boon [34] or Spring and Grout [23], they do not explicitly state that light is required for these reactions to occur.

$$\alpha\text{-}HgS \rightleftharpoons \gamma\text{-}Hg_3S_2Cl_2 \rightleftharpoons \alpha\text{-}Hg_3S_2Cl_2 \rightleftharpoons Hg_2Cl_2 \quad (4)$$

All these studies describe corderoite as a phase preceding the formation of calomel during the alteration process. Indeed, thermodynamic modeling of the Hg, NaCl, H_2O containing system predicted the formation of corderoite (Figs. 14, 15, 16), a mercury sulfo-chloride which has been detected by several other scholars on altered cultural heritage materials [36, 37]. In the experimental study however, corderoite has not been identified. Clearly, this difference is significant, and the lack of corderoite here requires additional investigations. Several possible explanations are, therefore, explored.

The pH of the saline solution for example during artificial weathering may explain the presence or absence of particular compounds, and some phases are more stable than others. Parks and Nordstrom [52] predicted that corderoite will occur only under acidic conditions, and thermodynamic modeling carried out in this study partially supported these findings. Corderoite was only predicted to occur for the conditions where pH was below 8. The presence of small amounts of unreacted $Ca(OH)_2$, within the *fresco* mock-up blocks used in this experiment, created an alkaline environment during the artificial weathering

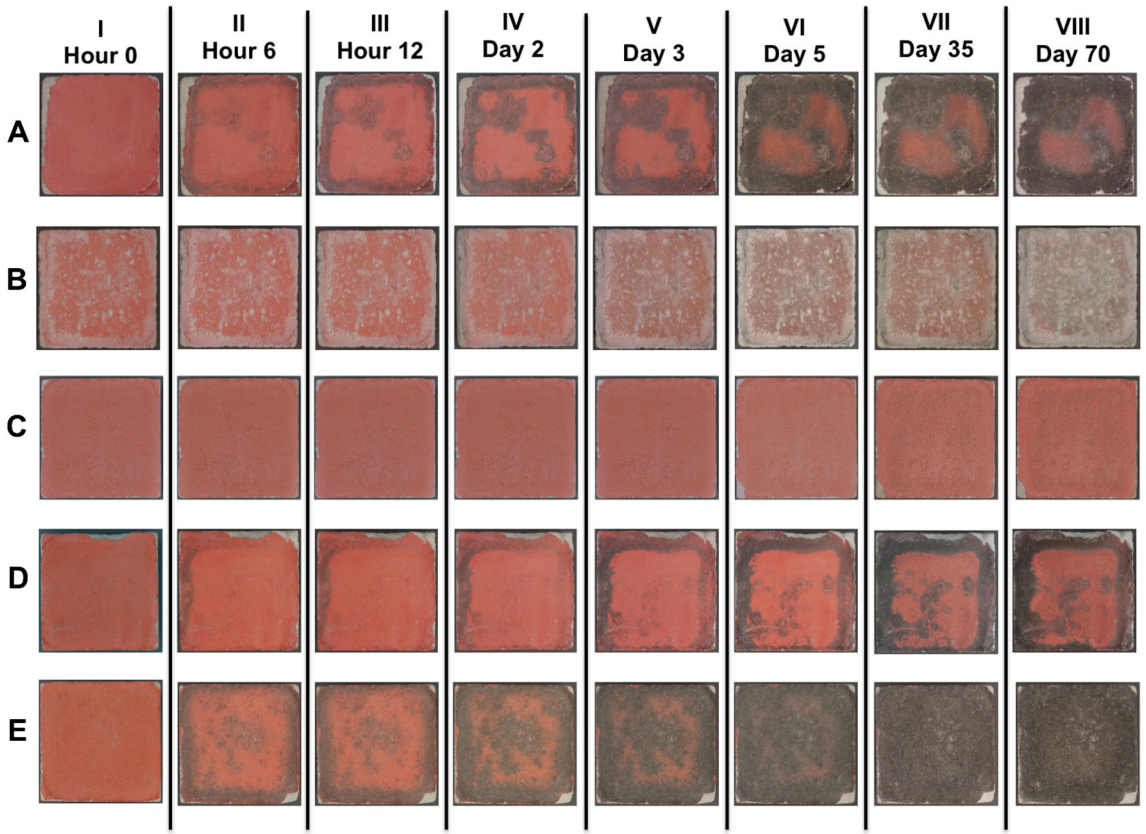

Fig. 13 Images of fresco mock-up blocks during the 70-day period of light exposure in a windowsill at the Getty Villa in Malibu, CA. a[*1–VIII*]: Exposed to 0.1 M NaCl solution, dried in dark prior to light exposure; **b**[1–VIII]: Exposed to 5 M NaCl solution, dried in dark prior to light exposure; **c**[*1–VIII*]: Exposed to 0.1 M NaCl solution; **d**[*1–VIII*]: Exposed to 0.1 M NaCl solution, allowed to partially dry, desalinated, and finally exposed to light; **e**[1–VIII]: Exposed to 5 M NaCl solution, allowed to partially dry, desalinated, and finally exposed to light

process. The pH of saline solutions changed from 7 when blocks were first placed in contact with solution to 12 after 12 h of contact with the solution. This suggests that the unreacted $Ca(OH)_2$ was present within the block and eventually came into equilibrium with aqueous phase subsequently resulting in elevated pH. However, experiments carried out by Radepont [29], in which NaOCl with pH 12 was used as the chlorine source, formed corderoite, thus indicating that an acidic environment, as predicted in some thermodynamic models, is not the determining factor for its formation. Therefore, the lack of detection may be attributed to the timing of measurement after exposure to light, and it is possible that the formation of corderoite and calomel is time-sensitive. Corderoite could have been present for some period on the *fresco* blocks, but have gone undetected.

The presence of calomel both before and after light-induced blackening, as well as the inability to detect corderoite, indicates that color-shift observed during alteration cannot be attributed to the presence of either mercury chloride compounds.

4.2.2 Formation of metallic mercury

Formation of metallic mercury during photodegradation of cinnabar has been indicated in the past through the application of electrochemical methods [39]. The photosensitivity of calomel is well known as in the presence of light, calomel undergoes a disproportionation reaction [53] and degrades in black metallic mercury and in white mercury (II) chloride (Eq. 2).

The formation of metallic mercury is predicted by thermodynamic modeling to occur under certain conditions within the $HgS–NaCl–H_2O$ system. Attempts to visually observe metallic mercury on the surface of degraded particles using SEM were unsuccessful. Nor was there evidence of the "hot spots" which Keune and Boone [34] have suggested indicated the presence of metallic mercury on blackened particles. It should also be noted that mercury(II) chloride was untraceable by XRD on altered surfaces. However, another possibility is that the amount of material formed was below the instrument's detection limit. The fact that the blackening occurs at the time of

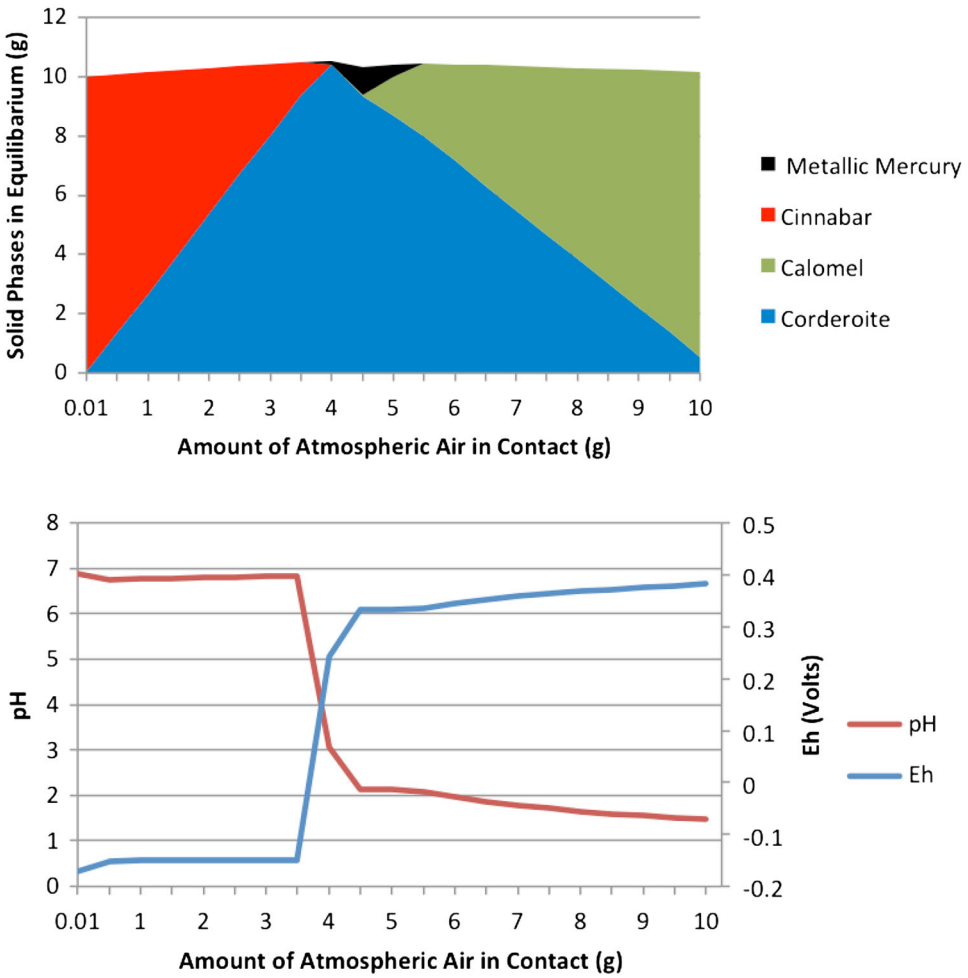

Fig. 14 *Top* Model showing changes in phase assemblage as a function of the amount of air being in contact with HgS mineral exposed to a 0.1 M NaCl solution; equilibration of HgS (10 g) with H_2O (1000 g) and NaCl (5.844 g) and various amounts of air (g). *Bottom* variation in pH aqueous phase and redox potential as a factor of amount of atmospheric air within the model

light exposure and the amorphization of the blackened particles can suggest that nanoparticle of metallic mercury can be also responsible for the color-shift from red to black. It should be clarified though that at the current state of knowledge, this is only the hypothesis as there is no experimental evidence of the presence of metallic mercury yet.

4.2.3 Calcium–sulfur-containing compounds

SEM–EDS analysis indicated the possible formation of a calcium–sulfur phase on the surface (Fig. 10b, d). The specific compound was not identified by XRD. It is possible that gypsum precipitated at very low quantities below the detection limit of the XRD technique (normally 3–5 wt%) and could be overpowered by large quantities of other phases present in the system such as calcite or cinnabar. However, the phase observed during SEM–EDS analysis is likely to be the very early stage of gypsum ($CaSO_4{\cdot}2H_2O$) formation at the *fresco* surface. This is a phenomenon predicted by thermodynamic modeling and previously observed in altered cinnabar on *fresco* samples recovered from Pompeii [19, 29, 36] and from the Santa Maria Church in Northern Spain [48]. Radepont et al. [37] also indicated the presence of gypsum in some of their samples; however, they were not able to demonstrate the formation of gypsum through their thermodynamic model. This is likely on the account of the fact that in their approach considering only Hg–S–Cl–H_2O they did not take into consideration the presence of other ions such as calcium which is abundant in wall paintings deriving both from the binder ($Ca(OH)_2$) and calcareous aggregates (i.e., marble dust). As demonstrated in the model present herein (Figs. 14, 15, 16), the presence or lack of $CaCO_3$/$Ca(OH)_2$ can significantly affect the conditions and regions of stability for gypsum precipitation. It is possible, however, that the existence of other ions such as K or any other impurities that are in contact with α-HgS can significantly affect the mineral nature and consequently phase equilibria of these systems.

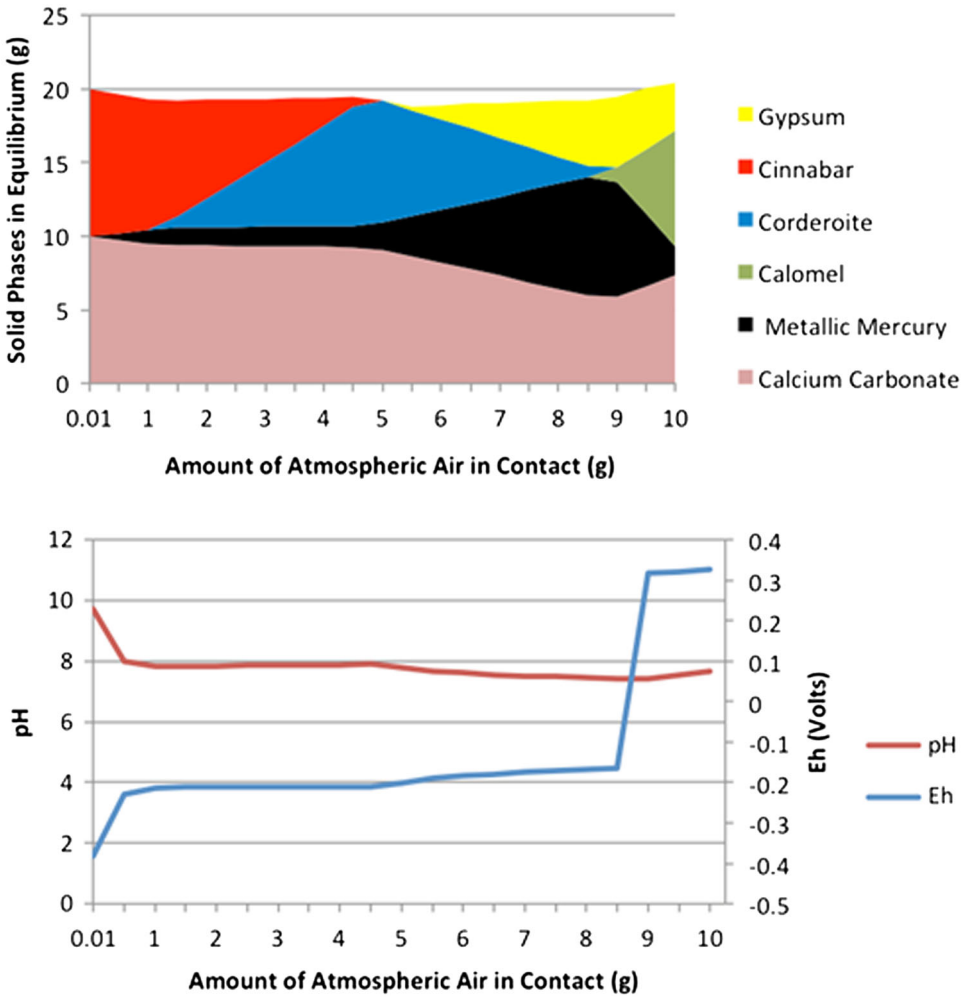

Fig. 15 *Top* Model showing changes in phase assemblage as a function of the amount of air being in contact with cinnabar pigment on fully carbonated fresco surface exposed to a 0.1 M NaCl solution; equilibration of HgS (10 g) and $CaCO_3$ (10 g) with H_2O (1000 g) and NaCl (5.844 g) and various amounts of air (g). *Bottom* variation in pH of aqueous phase and redox potential as a factor of amount of atmospheric air within the model

As proposed by Cotte et al. [19], it appears that sulfur lost by the cinnabar particles during the alteration process reacts with oxygen present in the environment (Eq. 5).

$$S + O_2 \rightarrow SO_2 \quad (5)$$

This SO_2 subsequently reacts with the $Ca(OH)_2/CaCO_3$ (*fresco* binder) at the surface to form gypsum (Eq. 6).

$$SO_2 + CaCO_3 + {}^1/_2O_2 + 2H_2O \rightarrow CaSO_4 \cdot 2H_2O + CO_2 \quad (6)$$

It is possible that external sources of SO_2, e.g., combustion product present in the environment, have in some cases played a role in the formation of gypsum on cinnabar-pigmented historic wall paintings or archaeological *frescoes* unearthed for extended periods, as has been documented on other calcareous cultural heritage monuments [41, 44–46]. However, the formation of calcium–sulfur compounds, under controlled conditions and in such a short time span, would suggest that the formation of gypsum is a by-product of the alteration process on calcium-based substrates and does not necessarily require an additional SO_2 source from an outside environment. Though not the primary source of blackening, the presence of fine dust particles trapped within the gypsum layer during formation likely exacerbates the darkening of cinnabar-pigmented calcium-based substrate of materials housed in an outdoor setting. Radepont et al. [37] reported that in laboratory-controlled experiments, gypsum was identified after 180 days. This suggests that though gypsum precipitation can be kinetically restrained, under certain conditions, it is a thermodynamically stable phase. This observation is supported by equilibrium predictions presented in this work (Figs. 15, 16).

4.3 Assessment of desalination and alternate drying methodology as blackening inhibitor

Efforts to inhibit or limit alteration through the implementation of alternate drying methodologies (drying in the dark to limit moisture at the time of light exposure) or the

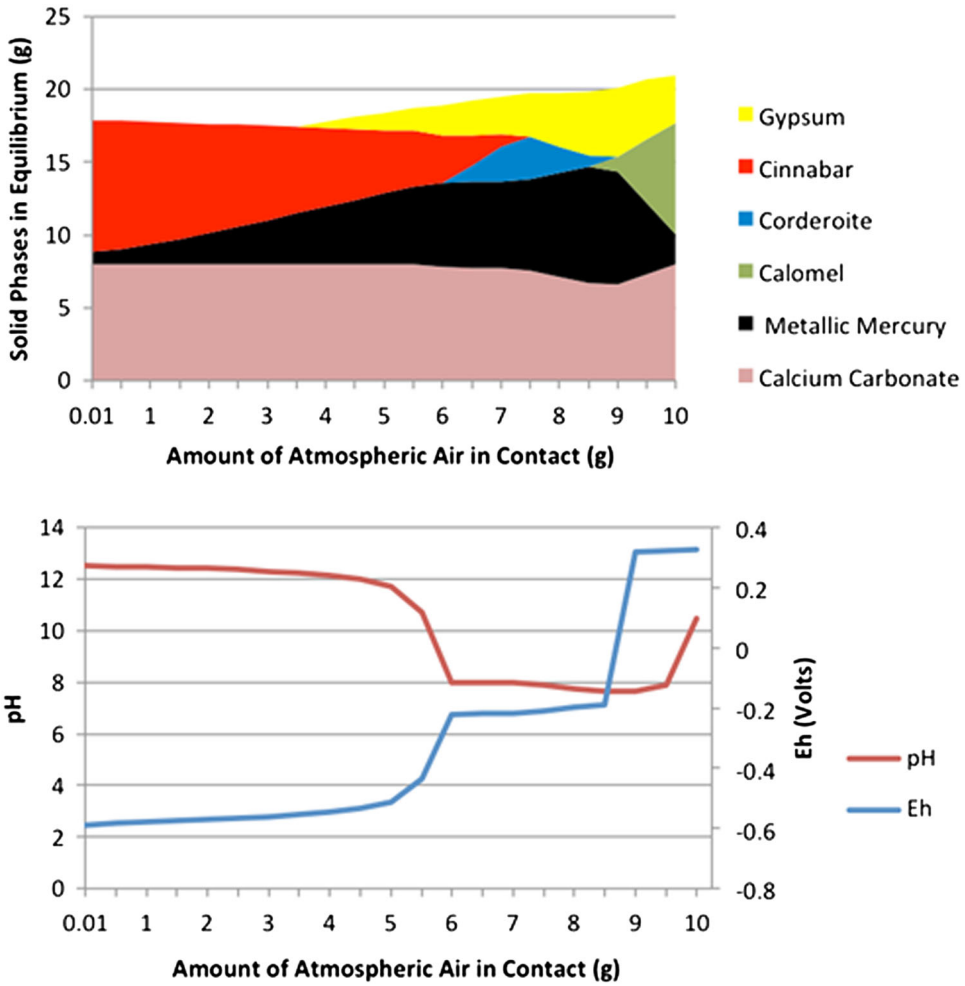

Fig. 16 *Top* Model showing changes in phase assemblage as a function of the amount of air being in contact with cinnabar pigment on recently constructed fresco surface—one that has not fully carbonated—which is exposed to a 0.1 M NaCl solution; equilibration of HgS (10 g) and 8 g $CaCO_3$ and 2 g of $Ca(OH)_2$ with H_2O (1000 g) and NaCl (5.844 g) and various amounts of air (g). It should be noted that at room temperature, the solubility of $Ca(OH)_2$ is approximately 2 g/L; therefore, the compound is predicted to fully dissolve in this scenario and only alter the pH of aqueous phase. *Bottom* variation in pH of aqueous phase and redox potential as a factor of amount of atmospheric air within the model

use of desalination procedures proved ineffectual. In fact, in some cases, the treatments carried out lead to increased rather than reduced darkening. It appears that these conservation treatments, which prolonged the period of contact with NaCl solutions with the cinnabar, create an environment conducive to the formation of calomel.

Letting the mock-up blocks to dry in the dark has significantly slowed down the rate of water evaporation. It took 14 days for those placed in the dark to come to a constant weight, while those placed directly under sunlight were dry after 3 days. This extended drying period in the absence of light allowed the cinnabar-pigmented surface to remain in contact with the NaCl solution for much longer than when blocks dried under direct sunlight. Repeated desalination attempts of the blocks with DI H_2O to remove the salts similarly resulted in prolonged contact of NaCl solutions; attempts to reduced salts required multiple sequences of poulticing leaving block exposed for $\sim$15 days. The solubility of calomel, while significantly higher than cinnabar, is quite low (0.2 mg/100 mL). Consequently, once the compound is formed, only a small portion may be dissolved and absorbed into the cellulosic fibers during the poulticing process though diffusion and advection processes. In case of trials carried out here, the rate of calomel formation appeared to surpass the rate at which it was removed.

Allowing blocks to dry prior to placing them into the light failed to limit darkening process. However, drying chlorine-contaminated cinnabar quickly and keeping the material under desiccating conditions appears to reduce and slow down blackening. In contrast, increasing relative humidity (RH) of the environment, dramatically accelerates blackening. Cinnabar pigment treated with 0.1 M NaCl solution and stored at $<$5 % RH showed no discernible darkening when placed in the light for 21 days, while pigment treated in the same manner and stored at $\sim$70 % RH showed significant blackening. The rate of reaction appears considerably reduced in the absence of moisture. It is possible that water acts as medium necessary to facilitate darkening reactions.

5 Conclusions

The experimental and theoretical research conducted in this study supports previous assertions that chlorine and light play pivotal roles in the blackening process of cinnabar and that moisture is another significant parameter contributing to the transformation processes. In the absence of these, the color change from red to black will not occur. However, the specific mechanism by which this transformation occurs is still not clearly understood. In contrast to previous studies, this research indicates that the processes and intermediate phases responsible for the chemical alteration of the cinnabar begin prior to light exposure. Calomel may occur in the absence of light. Therefore, while steps may be taken to limit the blackening of the surface, complete inhibition of the alteration process through drying of the *fresco* prior to light exposure or the removal of chlorine ions through poulticing has proven ineffectual. Equilibrium thermodynamics base predictions suggest that cinnabar darkening processes are complex and highly dependent on the redox potential, pH as well as abundance and concentrations of other ions present in the system.

Recommendations for conservators charged with the preservation of cinnabar-pigmented *frescos* are, therefore, limited. Tests for chloride salts should be conducted at the time of excavation to determine the risk of blackening. A variety of possible detection techniques are available including chloride test strips, colorimetric indicator kits, and microchemical tests, as well as instrumental analysis including chloride ion selective electrode, ion chromatography, XRF, and XRD. However, care must be taken to ensure that the testing methodology employed is adequately sensitive. Cinnabar-pigmented surfaces with >0.01 Cl wt% content should be considered as risk of alteration. Those conserving wall paintings after excavation must, additionally, note that industrial and natural sources, including chlorofluorocarbons and sea spray, present within the environment when in combination with elevated relative humidity could induce alteration at a later time.

As attempts to reduce the amount of Cl^- have proven ineffective at decreasing the risk of alteration, interventions should be focused on limiting light and moisture. Where chlorides are present, excavation should be carried out in the shade of a tent and light-blocking materials placed in front of cinnabar-pigmented surfaces, which are not currently under active excavation. Fragments that are found ex situ should be promptly removed from the ground and stored in a darkened environment. It may also be prudent to speed drying and subsequently house such dissociated materials with a desiccant to limit continued formation of Hg–Cl-containing compounds. However, it is important to understand that such a procedure could cause surface and subsurface efflorescence of other soluble salts causing visual and mechanical damage to the artifact. For this reason, such a treatment should only be carried out with caution and when all other parameters and risks have been carefully evaluated.

Acknowledgments All authors would like to acknowledge Molecular and Nano Archaeology Laboratory at UCLA.

References

1. P.W. Lehmann, *Roman Wall Paintings from Boscoreale in the Metropolitan Museum of Art* (Archaeological Institute of America, Cambridge, 1953)
2. J.R. Clarke, *The Houses of Roman Italy, 100 B.C.-A.D. 250: Ritual, Space, and Decoration* (University of California Press, Berkeley, 1991)
3. M. Bussagli, *Rome, Art and Architecture* (Könemann, Cologne, 1999)
4. A. Maiuri, *Roman Painting*. Trans. Stuart Gilbert (Skira, Geneva, Switzerland, 1953)
5. R. Ling, *Roman Painting* (Cambridge University Press, Cambridge, 1991)
6. E.M. Moormann, in *Functional and Spatial Analysis of Wall Painting*. Proceedings of the 5th International Congress on Ancient Wall Painting, Amsterdam, 8–12 September 1992 (Stichting Babesch, Leiden, 1993)
7. P. Mora, L. Mora, P. Philippot, *The Conservation of Wall Paintings* (Butterworth & Co., New York, 1984)
8. C. Arendt, in *The Role of Architectural Fabric in the Preservation of Wall Paintings*, ed. by S. Cather. The Conservation of Wall Paintings: Proceedings of a Symposium Organized by the Courtauld Institute of Art and the Getty Conservation Institute, London, July 13–16, 1987 (Getty Conservation Institute, Marina del Rey, CA, 1991)
9. A. Arnold, K. Zehnder, in *Monitoring Wall Paintings Affected by Soluble Salts*, ed. by S. Cather. The Conservation of Wall Paintings: Proceedings of a Symposium Organized by the Courtauld Institute of Art and the Getty Conservation Institute, London, July 13–16, 1987 (Getty Conservation Institute, Marina del Rey, CA, 1991)
10. M. Matteini, in *Review: An Assessment of Florentine Methods of Wall Painting Conservation Based on the Use of Mineral Treatments*. ed. by S. Cather, The Conservation of Wall Paintings: Proceedings of a Symposium Organized by the Courtauld Institute of Art and the Getty Conservation Institute, London, July 13–16, 1987 (Getty Conservation Institute, Marina del Rey, CA, 1991)
11. O. Ciferri, P. Tiano, G. Mastromei, *Of Microbes and Art: The Role of Microbial Communities in the Degradation and Protection of Cultural Heritage* (Kluwer Academic/Plenum Publishers, New York, 2000)
12. L. Dei, A. Ahle, P. Baglioni, D. Dini, E. Ferroni, Green degradation products of azurite in wall paintings: identification and conservation treatment. Stud. Conserv. **43**, 80–88 (1998)
13. S. Giovannoni, M. Matteini, A. Moles, Studies and developments concerning the problem of altered lead pigments in wall painting. Stud. Conserv. **35**, 33–51 (1990)
14. V. Daniels, R. Stacey, A. Middleton, The blackening of paint containing egyptian blue. Stud. Conserv. **49**, 217–230 (2004)
15. E. Minopoulou, A study of smalt and red lead discolouration in antiphonitis wall paintings in cyprus. Appl. Phys. Mater. Sci. Process. **96**, 701–711 (2009)

16. Pliny, *The Elder Pliny's Chapters on Chemical Subjects*, ed. by K.C. Bailey (E. Arnold & Co., London, UK, 1929)
17. Vitruvius, *The Ten Books on Architecture*. Tran. H. M. Morgan (Dover Publications, New York, 1960)
18. R.J. Gettens, R.L. Feller, W.T. Chase, in *'Vermillion and Cinnabar', In Artists' Pigments a Handbook of Their History and Characteristics*. ed. by R.L. Feller, A. Roy, E. West FitzHugh, B. Hepburn Berrie (National Gallery of Art, Washington, 1986)
19. M. Cotte, J. Susini, N. Metrich, A. Moscato, C. Gratziu, A. Bertagnini, M. Pagano, Blackening of Pompeian cinnabar paintings: X-ray microspectroscopy analysis. Anal. Chem. **78**, 7484–7492 (2006)
20. R.L. Feller, *Studies on the Darkening of Vermilion by Light*. Report and Studies in the History of Art (National Gallery of Art, Washington, DC, 1967)
21. R.J. Gettens, R.L. Feller, W.T. Chase, Vermilion and cinnabar. Stud. Conserv. **17**, 45–69 (1972)
22. V. Daniels, R. Stacey, A. Middleton, in *'The Blackening of Vermillion by Light', In Recent Advances in Conservation and Analysis of Artifacts.* ed. by J. Black (Summer School Press, London, UK, 1987)
23. M. Spring, R. Grout, The blackening of vermilion: an analytical study of the process in paintings. Natl. Gallery Tech. Bull. **23**, 50–61 (2002)
24. R. Grout, A. Burnstock, A study of the blackening of vermilion. Zeitschrift für Kunsttechnologie und Konservierung **141**, 15–22 (2000)
25. I. Istudor, A. Dina, G. Rosu, D. Seclaman, G. Niculescu, An alteration phenomenon of cinnabar red pigment in mural paintings from sucevita. E_Conservation **2**, 24–33 (2007)
26. F.W. Dickson, G. Tunell, The stability of cinnabar and metacinnabar. Am. Minerol. **44**, 471–487 (1959)
27. J.K. McCormack, The darkening of cinnabar in sunlight. Miner. Deposita **35**, 796–798 (2000)
28. J.K. McCormack, *Mercury Sulf-Halide Minerals and Crystalline Phases, and Experimental Formation Conditions, in the System* $Hg_3S_2Cl_2$–$Hg_3S_2Br_2$–$Hg_3S_2I_2$ (Thesis (Ph. D.)-University of Nevada, Reno, 1997)
29. M. Radepont, *Understanding of Chemical Reactions Involved in Pigment Discoloration, in Particular in Mercury Sulfide (HgS) Blackening* (PhD thesis, Universiteit Antwerpen, 2013)
30. F. Da Pieve, C. Hogan, D. Lamoen, J. Verbeeck, F. Vanmeert, M. Radepont, M. Cotte, K. Janssens, X. Gonze, G. Van Tendeloo, Casting light on the darkening of colors in historical paintings. Phys. Rev. Lett. **111** (2013). doi:10.1103/PhysRevLett.111.208302
31. H. Béarat, Chemical and mineralogical analyses of Gallo-Roman wall painting from Dietikon, Switzerland. Archaeometry **38**, 81–95 (1996)
32. J.K. McCormack, F.W. Dickson, M.P. Leshendok, Radtkeite, Hg 3 S 2 ClI, a new mineral from the McDermitt mercury deposit, Humboldt County, Nevada. Am. Mineral. **76**, 1715–1721 (1991)
33. R.S. Davidson, C.J., Willsher C.J., The Light-induced Blackening of Red Mercury (II) Sulphide. *Journal of the Chemical Society* **1981,** *Dalton Transactions 3*, 833-835
34. K. Keune, J.J. Boon, Analytical imaging studies clarifying the process of the darkening of vermilion in paintings. Anal. Chem. **77**, 4742–4750 (2005)
35. M. Cotte, J. Susini, J. Dik, K. Janssens, Synchrotron-based X-ray absorption spectroscopy for art conservation: looking back and looking forward. Acc. Chem. Res. **46**, 705–714 (2010)
36. M. Radepont, W. de Nolf, K. Janssens, G. Van der Snickt, Y. Coquinot, L. Klaassen, M. Cotte, The use of microscopic X-ray diffraction for the study of HgS and its degradation products corderoite, kenhsuite and calomel in historical paintings. J. Anal. At. Spectrom. **26**, 959–968 (2011)
37. M. Radepont, Y. Coquinot, K. Janssens, J. Ezrati, W. de Nolf, M. Cotte, Thermodynamic and experimental study of the degradation of the red pigment mercury sulfide. J. Anal. At. Spectrom. **30**, 599–612 (2015)
38. M. Cotte, J. Susini, V.A. Solé, Y. Taniguchi, J. Chillida, E. Checroun, P. Walter, Applications of synchrotron-based microimaging techniques to the chemical analysis of ancient paintings. J. Anal. At. Spectrom. **23**, 820–828 (2008)
39. W. Anaf, K. Janssens, K. De Wael, Formation of metallic mercury during photodegradation/photodarkening of a-HgS: electrochemical evidence. Angew. Chem. **125**, 12800–12803 (2013)
40. K.L. Gauri, A.N. Chowdhury, N.P. Kulshreshtha, A.R. Punuru, The sulfation of marble and the treatment of gypsum crusts. Stud. Conserv. **34**, 201–206 (1989)
41. P. Ausset, R. Lefevre, J. Philippon, C. Venet, in *Large-Scale Distribution of Fly-Ash Particles Inside Weathering Crusts on Calcium Carbonate Substrates: Some Examples on French Monuments*, ed. by D. Decrouez, J. Chamay, F. Zezza. La Conservation des Monuments dans le Basin Méditerranéen: Actes du 2ème Symposium International = The Conservation of Monuments in the Mediterranean Basin: Proceedings of the 2nd International Symposium (Ville de Geneve, Museum d'histoire naturelle, and Muse d'art et d'histoire., Geneva, 1992), pp. 121–139
42. V. Fassina, in *Atmospheric Pollutants Responsible for Stone Decay: Wet and Dry Surface Deposition of Air Pollutants on Stone and the Formation of Black Scabs*, ed. by F. Zezza. Weathering and Air Pollution: Primo Corso Della Scuola Universitaria C.U.M. Conservazione dei Monumenti, Lago di Garda (Portese), Venezia, Milano, 2–9 Settembre 1991 (Mario Adda Editore, Bari, 1992), pp. 67–86
43. M. Tennikat, Blumenkohl-, Sinter-und Seidenglanzkruste: Salzkartierung und naturwissenschaftliche Erklärungen. *Forschungsprojekt Wandmalerei-Schäden: ein Förderprojekt des Bundesministers für Forschung und Technologie: Schlußbericht zu den interdisziplinären Befunden. Niedersächsisches Landesverwaltungsamt,* 1994, pp. 99–108
44. A.E. Charola, R. Ware, in *Acid Deposition and the Deterioration of Stone: A Brief Review of a Broad Topic*, ed by S. Siegesmund, T. Weiss, A. Vollbrech. Natural Stone, Weathering Phenomena, Conservation Strategies and Case Studies, Geological Society Special Publications 205 (Geological Society of London, London, 2002), pp. 393–406
45. A.E. Charola, J. Pühringer, M. Steiger, Gypsum: a review of its role in the deterioration of building materials. Environ. Geol. **52**, 339–352 (2007)
46. L. Toniolo, C.M. Zerbi, R. Bugini, Black layers on historical architecture. Environ. Sci. Pollut. Res. **16**, 218–226 (2009)
47. F.E. Doehne, C.A. Price, in *Stone Conservation: An Overview of Current Research* (Getty Conservation Institute, Los Angeles, California, 2010)
48. M. Perez-Alanso, K. Castro, M. Alvarez, J.M. Madariaga, Investigation of degradation mechanisms by portable Raman spectroscopy and thermodynamic speciation: the wall paining of Santa Maria de Lemoniz (Basque County, North of Spain). Anal. Chim. Acta. **571**, 121–128 (2006)
49. R.M. Dreyer, Darkening of Cinnabar in Sunlight. Am. Mineral. **23**, 796–798 (1938)
50. R. Johnston-Feller, *Color science in the Examination of Museum Objects Nondestructive Procedures* (Getty Conservation Institute, Los Angeles, 2001)

51. D. Kulik, U. Berner, E. Curti, Modelling chemical equilibrium partitioning with the GEMS-PSI code, vol 4. PSI Scientific Report, http://gems.web.psi.ch. 2003, pp. 109–122
52. G.A. Parks, D.K. Nordstrom, Estimated free energies of formation, water solubilities, and stability fields for schuetteite (Hg3O2SO4) and corderoite (Hg3S2Cl2) at 298 K. Chem. Model. Aqueous Syst. **93**, 339–352 (1979)
53. C.J. Barta, Z. Bryknar, M. Procio, Photosensitivity of mercurous chloride single crystals in 280–400 nm spectral region. Czechoslovak J. Phys. B **37**, 1301–1310 (1987)